

Poly(N-hydroxyethyl acrylamide) / Chitosan Based Hydrogels

Ehsan Bahramzadeh

Submitted to the
Institute of Graduate Studies and Research
in partial fulfillment of the requirements for the degree of

Doctor of Philosophy
in
Chemistry

Eastern Mediterranean University
January 2019
Gazimağusa, North Cyprus

Approval of the Institute of Graduate Studies and Research

Assoc. Prof. Dr. Ali Hakan Ulusoy
Acting Director

I certify that this thesis satisfies all the requirements as a thesis for the degree of Doctor of Philosophy in Chemistry.

Prof. Dr. Izzet Sakallı
Chair, Department of Chemistry

We certify that we have read this thesis and that in our opinion it is fully adequate in scope and quality as a thesis for the degree of Doctor of Philosophy in Chemistry.

Prof. Dr. Elvan Yılmaz
Supervisor

Examining Committee

1. Prof. Dr. Nesrin Hasırcı
2. Prof. Dr. Hayal Bülbül Sönmez
3. Prof. Dr. Elvan Yılmaz
4. Assoc. Prof. Dr. Terin Adalı
5. Assoc. Prof. Dr. Mustafa Gazi

ABSTRACT

Poly(N-hydroxyethyl acrylamide) (polyHEAA) was grafted onto chitosan in aqueous acidic medium using potassium per sulphate initiator to obtain polymer surfaces with blood compatibility for potential biomedical applications such as blood contacting devices as artificial veins or devices to remove excess ions from the blood. The grafting parameters monomer concentration, crosslinker concentration, initiator concentration, processing time and temperature were changed to find out the effect of each parameter on the grafting yield (%G) and choose the best preparation parameters for the aimed purpose. Grafting yield values up to 600% were achieved. Thermally cross-linked products were obtained upon drying at 60°C overnight. Chemically cross-linked films were prepared using methylene bis acrylamide (MBA) and glutaraldehyde (GA) cross-linkers. The products were characterized by FTIR, XRD and SEM analyses. Blood compatibility and protein adsorption characteristics of the MBA crosslinked and poly (N-hydroxy ethyl acrylamide) grafted chitosans namely (chitosan-*graft*-polyHEAA;MBA) were investigated. Protein adsorption onto the film surfaces were about 10% human serum albumin (HSA) removal from aqueous solution, after 3 h contact, *in vitro*. Blood compatibility was evaluated with respect to activated prothrombin time (PT), activated partial thromboplastin time (APTT), and platelet adhesion. PT and APTT values remained within normal ranges after blood-polymer contact for 90 minutes, with chitosan-*graft*-polyHEAA films, *in vitro*. Examining chitosan-*graft*-MBA or chitosan-*graft*-(polyHEAA;MBA), and blank chitosan films caused higher PT and APTT values under similar experimental conditions with chitosan-*graft*-polyHEAA films, exhibiting blood anticoagulant activity. SEM images taken before and after contact with blood sample did not reveal

any significant blood component adhesion on the chitosan-*graft*-(polyHEAA;MBA) film surface contrary to the observation made on the chitosan film. However, the blood components on the film surfaces were not identified.

Glutaraldehyde crosslinked films (chitosan-*graft*-(polyHEAA;GA)) were prepared and tested as adsorbents for Fe³⁺ ion in solution. It was observed that crosslinking, swelling and polyHEAA grafting values acted together in determining the adsorption capacity. The highest adsorption capacity was found as 44.8 mg Fe /g adsorbent at pH=1.2, at room temperature from 500 ppm FeCl₃ solution within 24 h contact by a sample with 586% grafting yield value.

Keywords: biomaterial, chitosan, glutaraldehyde, grafting, hemocompatibility, hydrogel, methylene bis acrylamide, polyacrylamide

ÖZ

Bu çalışmada, sulu, asitli ortamda kitosan üzerine poli(N-hidroksietil akrilamid) aşılama konu edilmiştir. Çalışmanın amacı kan uyumluluğuna sahip polimer yüzeyler elde etmektir. Bu amaçla, öncelikle poli(N-hidroksi etil akrilamid) polimerinin kitosan üzerine aşılama koşulları incelenmiştir. Monomer, başlatıcı, çapraz bağlayıcı derişimlerinin ve sıcaklık ile zamanın yüzde aşılama (%G) değerleri üzerindeki etkileri gravimetrik yöntemle belirlenmiş ve en yüksek aşılama yüzdesinin elde edildiği optimum koşullar belirlenmiştir. Kimyasal çapraz bağlayıcının bulunmadığı durumlarda ısıl işlem sonucu çapraz bağlı ürünler elde edilmiştir. Kimyasal çapraz bağlayıcı olarak metilen bis akrilamid (MBA) ile glutaraldehit (GA) kullanılmıştır. MBA ile çapraz bağlanmış ürünlerin (kitosan-*aşı*-poli(N-hidroksi etil akrilamid;MBA) kan uyumluluğu ve protein (HSA) adsorplama davranışları incelenmiştir. Buna göre (kitosan-*aşı*-poli(N-hidroksi etil akrilamid;MBA) filmlerin HSA adsorplama özelliklerinin birbirinden anlamlı bir farklılık göstermediği ve çözeltideki HSA konsantrasyonun filmlerle üç saatlik bir etkileşimden sonra ortalama %10'luk değerinde bir düşüşe uğradığı gözlemlenmiştir. Kan uyumluluğu deneyleri PT ve APTT değerlerinin yalnızca ısıl işlemle çapraz bağlanmış olan polimer filmleri (kitosan-*aşı*-polyHEAA) ile doksan dakikalık etkileşim sonucunda normal sınırlar içinde kaldığı saptanmıştır. Buna karşın kitosan-*aşı*-MBA or kitosan-*aşı*-(polyHEAA;MBA), ve kitosan filmleri ile etkileşimden sonra kanın PT ve APTT değerlerinin yükseldiği ve bu malzemelerin antikoagulan etkisi gösterdikleri belirlenmiştir. Bunun yanında, SEM fotoğrafları poliHEAA aşılama film yüzeyinin kanla etkileşim sonrasında kitosana göre daha temiz kaldığını göstermiştir. Ancak yüzeydeki kan bileşenleri tanımlanamamıştır.

Glutaraldehit ile apraz baėlanmıř ve poli(N-hidrprksi etil akrilamid) ile ařılanmıř filmlerin, kitosan-*graft*-(polyHEAA;GA), ise özeltiden Fe³⁺ iyonu adsorplama davranıřları incelenmiřtir. Oda sıcaklıėında elde edilen ve mg Fe/g polimer cinsinden hesaplanan adsorplama kapasitesi deėerlerine gre apraz baėlanma miktarı dengedeki %řiřme deėeri ile % ařılanma deėerlerinin adsorplama kapasitesini etkilediėi sonucuna varılmıřtır. En yksek demir adsorplama kapasitesine sahip rneėin pH=1.2 ve oda sıcaklıėında 44.8 mg Fe/g polimer deėeri ile %586'lık ařılanma ve %190'lık řiřme deėerlerine sahip olan rnek olduėu belirlenmiřtir.

Anahtar Kelimeler: ařı polimerleřme, biyomalzeme, glutaraldehit, hidrojel, kitosan, kan uyumluluėu, metilen bis akrilamid, poliakrilamid

DEDICATION

Dedicated with affection
to my parents
who make everything worthwhile

ACKNOWLEDGMENT

I would like to express sincere appreciation to my advisor Prof. Dr. Elvan Yilmaz for her continuous support of my Ph.D study, for her immense knowledge, patience and motivation. Her guidance in all the time of study and writing of this thesis helped me. I feel very lucky to have Prof. Dr. Elvan Yilmaz as advisor for my Ph.D study and I wish she always shines.

Many thanks also go to Assoc. Prof. Dr. Terin Adali for her precious support. She kindly provided me an opportunity to join her research team and facilities.

I would also like to thank the rest of my monitoring committee members, Prof. Dr. Osman Yilmaz and Assoc. Prof. Dr. Mustafa Gazi whom their experience and comments throughout the thesis always kept me in a right way.

Dear Prof. Dr. Gonul Sahin, Dr Zulal Yalinca, Dr Tugba Ercetin, Dr. Mohammad Shaker, Amir H. Fallah, Reihaneh Behnoush thank you very much for your support, effective involvement and understanding.

I couldn't have imagined having better labmates than EMU Chemistry and Pharmacy students (Salam A. Basheer, Muhamad Y. Magaji, Tooraj Poorhassan Asliardeh and Mostafa Farhadi) during my thesis research, for the sleepless nights we were working together, and for all the fun we had.

TABLE OF CONTENTS

ABSTRACT.....	iii
ÖZ.....	v
DEDICATION.....	vii
ACKNOWLEDGMENT.....	viii
LIST OF TABLES.....	xii
LIST OF FIGURES.....	xiv
1 INTRODUCTION.....	1
1.1 General Properties of Biomaterials.....	1
1.1.1 Blood Compatibility.....	1
1.1.1.1 Conditions for Blood Compatible Materials.....	1
1.1.1.2 Host Response to Materials.....	3
1.1.1.3 Protein Adsorption onto Biomaterials.....	3
1.1.1.4 Cell – Biomaterial Interactions.....	3
1.1.1.5 Hemocompatibility Tests.....	4
1.2 Polymers as Biomedical Materials.....	5
1.3 Grafting: Polymer Modification for Biomedical Applications.....	6
1.3.1 Graft Copolymerization.....	7
1.3.2 Optimization of Grafting Parameters.....	8
1.4 Chitosan.....	8
1.4.1 Blood Compatibility of Chitosan and Chitosan Derivatives.....	10
1.4.2 Chitosan: Fe ³⁺ Adsorbent for Biomedical Applications.....	11
1.5 Poly (N-hydroxy ethyl acrylamide).....	12
1.5.1 Biomedical Properties of the Homopolymer and Copolymers of HEAA.....	13

1.6 Aims and Scope of the Thesis.....	13
2 EXPERIMENTAL.....	15
2.1 Materials	15
2.2 Equipment.....	15
2.3 Method.....	16
2.3.1 Grafting of Poly(N-hydroxyethyl acrylamide) onto Chitosan under Homogeneous Conditions.....	16
2.3.2 Preparation of Films for Blood Compatibility Tests.....	18
2.3.3 Synthesis of Chitosan-graft-(polyHEAA; GA) Films	19
2.3.4 Swelling Kinetics	20
2.3.5 <i>In-vitro</i> Coagulation Test Analyses	21
2.3.6 <i>In-vitro</i> Blood Contact Test	22
2.3.7 Human Serum Albumin (HSA) Adsorption	22
2.3.8 Fe ³⁺ Adsorption on Chitosan-graft-(polyHEAA; GA) Films	22
3 RESULTS AND DISCUSSION.....	24
3.1 Optimization of Grafting Parameters.....	24
3.1.1 FTIR Analysis.....	28
3.1.2 XRD Analysis	32
3.1.3 SEM Analysis	34
3.1.4 Swelling Behaviour of Chitosan-graft-polyHEAA and Chitosan-graft-(polyHEAA;MBA) Films	36
3.1.5 <i>In vitro</i> Coagulation Test Analyses.....	40
3.1.6 <i>In vitro</i> Blood Contact Test.....	47
3.1.7 Human Serum Albumin (HSA) Adsorption	50
3.2 Chitosan-graft-(PHEAA; GA) Films.....	52

3.2.1 FT-IR Analysis of Chitosan- <i>graft</i> -(PHEAA; GA).....	53
3.2.2 XRD Analysis of Chitosan- <i>graft</i> -(PHEAA; GA)	54
It has an amorphous nature.	54
3.2.3 SEM Analysis for Chitosan- <i>graft</i> -(PHEAA; GA)	54
3.2.4 Elemental Analysis of Chitosan- <i>graft</i> -(PHEAA; GA).....	56
3.2.5 Swelling Behaviour of Chitosan- <i>graft</i> -polyHEAA and Chitosan- <i>graft</i> - (polyHEAA;GA) Films.....	57
3.2.6 Iron (Fe ³⁺) Adsorption	67
3.2.6.1 SEM Analysis for Fe ³⁺ Adsorption.....	76
4 CONCLUSION.....	77
5 FUTURE DIRECTIONS	78
REFERENCES	79
APPENDIX.....	89
Appendix A: Ethical Consent	90

LIST OF TABLES

Table 1: Synthesis of chitosan- <i>graft</i> -polyHEAA in aqueous solution.....	17
Table 2: Synthesis of chitosan- <i>graft</i> -polyHEAA and chitosan- <i>graft</i> (polyHEAA;MBA) Films*	19
Table 3: Synthesis of hitosan- <i>graft</i> -(PHEAA; GA) Films characterization	20
Table 4: Synthesis of chitosan- <i>graft</i> -polyHEAA in aqueous solution *.....	26
Table 5: Synthesis of chitosan- <i>graft</i> -polyHEAA and chitosan- <i>graft</i> - (polyHEAA;MBA) Films*	28
Table 6: Swelling behavior over time for F7: chitosan- <i>graft</i> -(polyHEAA;MBA) (%G=406), F8: chitosan- <i>graft</i> -MBA (%G=86.6%), F11: chitosan- <i>graft</i> -polyHEAA (%G=333%), F12: blank chitosan at pH 7.4.....	37
Table 7: A) prothrombin time B) international normalized ratio C) PT percent D) activated partial thromboplastin time for F7: chitosan- <i>graft</i> -(polyHEAA;MBA) (%G=406), F8: chitosan- <i>graft</i> -MBA (%G=86.6%), F9: chitosan- <i>graft</i> -polyHEAA (%G=313%) F11: chitosan- <i>graft</i> -polyHEAA (%G=333%), F12: blank chitosan.....	43
Table 8: Spectrophotometric data for HSA adsorption.....	50
Table 9: HSA Adsorption capacities of the chitosan- <i>graft</i> -polyHEAA samples at 3h contact	52
Table 10: Synthesis of chitosan- <i>graft</i> -(PHEAA; GA) Films at 50°C	52
Table 11: Elemental analysis (Weight %) of chitosan- <i>graft</i> -(PHEAA; GA) samples (G1, G4, G9)	57
Table 12: Swelling behavior over time for G1, chitosan- <i>graft</i> -(polyHEAA;GA) (%G=226), G2, chitosan- <i>graft</i> -(polyHEAA;GA) (%G=586%), G3, chitosan- crosslinked-GA (%G=40), G4, chitosan- <i>graft</i> -(polyHEAA;GA) (%G=213), G5,	

chitosan-*graft*-(polyHEAA;GA) (%G=633), G6, chitosan-crosslinked-GA (%G=73.3), G7, chitosan-*graft*-polyHEAA (%G=173%), G8, chitosan-*graft*-polyHEAA (%G=440), G9, blank chitosan at pH 7.4 58

Table 13: Adsorbed mass (mg) of Fe³⁺ for G1: chitosan-*graft*-(polyHEAA;GA) (%G=226), G2: chitosan-*graft*-(polyHEAA;GA) (%G=586%), G3: chitosan-crosslinked-GA (%G=40), G4: chitosan-*graft*-(polyHEAA;GA) (%G=213), G5: chitosan-*graft*-(polyHEAA;GA) (%G=633), G6: chitosan-crosslinked-GA (%G=73.3), G7: chitosan-*graft*-polyHEAA (%G=173%), G8: chitosan-*graft*-polyHEAA (%G=440), G9: blank chitosan 68

Table 14: Grafting percentages, swelling percentages and Iron adsorption capacities for G1: chitosan-*graft*-(polyHEAA;GA) (%G=226), G2: chitosan-*graft*-(polyHEAA;GA) (%G=586%), G3: chitosan-crosslinked-GA (%G=40), G4: chitosan-*graft*-(polyHEAA;GA) (%G=213), G5: chitosan-*graft*-(polyHEAA;GA) (%G=633), G6: chitosan-crosslinked-GA (%G=73.3), G7: chitosan-*graft*-polyHEAA (%G=173%), G8: chitosan-*graft*-polyHEAA (%G=440), G9:chitosan 75

LIST OF FIGURES

Figure 1: Blood compatibility assessment (adapted from ISO-10993-4:2002(E)).....	5
Figure 2: Classification of natural polymers.....	6
Figure 3: Chemical structure and main characteristics of chitosan.....	10
Figure 4: Poly (N-hydroxy ethyl acrylamide).....	13
Figure 5: (A) chitosan-graft-(polyHEAA;MBA) film and (B) chitosan-graft-(polyHEAA;MBA) powder	25
Figure 6: FTIR spectrum of a) chitosan, b) polyHEAA, c) chitosan-graft-polyHEAA (S8), d) chitosan-graft-(polyHEAA;MBA) (S15).....	30
Figure 7: Proposed structure for chitosan-graft-(polyHEAA;MBA).....	31
Figure 8: XRD pattern of F7: chitosan-graft-(polyHEAA;MBA) (%G=406), F8: chitosan-graft-MBA (%G=86.6%), F9: chitosan-graft-polyHEAA (%G=313%) F11: chitosan-graft-polyHEAA (%G=333%), F12: chitosan.....	33
Figure 9: SEM picture of A) S15: chitosan-graft-(polyHEAA;MBA) powder, B) S16: chitosan-graft-MBA powder, C) F7: chitosan-graft-(polyHEAA;MBA), F8: chitosan-graft-MBA, F11: chitosan-graft-polyHEAA, and F12: chitosan (F12) film	35
Figure 10: Swelling behavior over time for A) F7: chitosan-graft-(polyHEAA;MBA) (%G=406), B) F8: chitosan-graft-MBA (%G=86.6%), C) F11: chitosan-graft-polyHEAA (%G=333%), D) F12: chitosan at pH 7.4	40
Figure 11: A) prothrombin time, B) international normalized ratio, C) PT percent, D) activated partial thromboplastin time for F7: chitosan-graft-(polyHEAA;MBA) (%G=406), F8: chitosan-graft-MBA (%G=86.6%), F9: chitosan-graft-polyHEAA (%G=313%) F11: chitosan-graft-polyHEAA (%G=333%), F12: blank chitosan.....	46

Figure 12: SEM images of A) chitosan-graft-(polyHEAA;MBA) film, B) chitosan-graft-(polyHEAA;MBA) film after contact with blood, C) chitosan, D) chitosan film after contact with blood.	49
Figure 13: FTIR spectrum of (a) chitosan (b) PHEAA (c) chitosan-graft-PHEAA (d) chitosan-graft-(PHEAA; GA).....	53
Figure 14: XRD analysis for b) Chitosan-graft-(PHEAA; GA)	54
Figure 15: SEM images (5000X) of G2) chitosan-graft-(polyHEAA;GA) (%G=586%), G4) chitosan-graft-(polyHEAA;GA) (%G=213), G5) chitosan-graft-(polyHEAA;GA) (%G=633), G7) chitosan-graft-polyHEAA (%G=173%), G9) chitosan.	55
Figure 16: elemental analysis for a) G1: chitosan-graft-(PHEAA; GA), b) G4: chitosan-graft-(PHEAA; GA), c) G9: chitosan.....	56
Figure 17: Swelling behavior over the time for a) G1: chitosan-graft-(polyHEAA;GA) (%G=226), b) G2: chitosan-graft-(polyHEAA;GA) (%G=586%), c) G3: chitosan-crosslinked-GA (%G=40), d) G4: chitosan-graft-(polyHEAA;GA) (%G=213), e) G5: chitosan-graft-(polyHEAA;GA) (%G=633), f) G6: chitosan-crosslinked-GA (%G=73.3), g) G7: chitosan-graft-polyHEAA (%G=173%), h) G8: chitosan-graft-polyHEAA (%G=440), i) G9: chitosan at pH 7.4	66
Figure 18: calibration curve for Iron solutions	67
Figure 19: Adsorbed mass (mg) of Fe ³⁺ for G1: chitosan-graft-(polyHEAA;GA) (%G=226), G2: chitosan-graft-(polyHEAA;GA) (%G=586%), G3: chitosan-crosslinked-GA (%G=40), G4: chitosan-graft-(polyHEAA;GA) (%G=213), G5: chitosan-graft-(polyHEAA;GA) (%G=633), G6: chitosan-crosslinked-GA (%G=73.3), G7: chitosan-graft-polyHEAA (%G=173%), G8: chitosan-graft-polyHEAA (%G=440), G9: chitosan.....	74

Figure 20: SEM images (5000X) of (a) chitosan-graft-(PHEAA; GA), (b) Fe³⁺ adsorbed chitosan-graft-(PHEAA; GA)..... 76

Chapter 1

INTRODUCTION

1.1 General Properties of Biomaterials

Biomaterials are identified by physical properties such as shape, surface and size. Their mechanical properties are characterized by measuring their fatigue, hardness, fracture toughness, elastic modulus values. Their surface properties include surface tension, morphology, and chemical functionalities present. Chemical properties exert a major effect over the interaction with cells and hence play an important role on the materials' *in vivo* performance [1].

1.1.1 Blood Compatibility

Materials to be tolerated in blood stream must be blood compatible.

1.1.1.1 Conditions for Blood Compatible Materials

Blood compatible materials are needed for biomedical applications, which involve either short term or long term blood-material contact. Blood detoxification devices are examples to short term blood-material contact. Artificial heart valves and blood vessels are in contact with blood for long periods of time.

Blood–material interactions involve complex mechanisms and depend both on materials properties and blood characteristics. Hemocompatibility can be described in various ways. It may be given by using a broader definition as the tolerance of blood to foreign material [2] or may more specifically be defined in terms of the ability of the material not to induce coagulation and inflammation upon contact with

normal blood [3]. On the other hand, Gorbet and Sefton [4] made another definition and proposed that blood compatibility is related to thrombosis that will induce blood coagulation.

When a polymeric material is considered, in general electrically neutral, hydrophilic polymers bearing hydrogen-bond acceptor groups exhibit blood compatibility better than others [5]. Hence, a hemocompatible polymer should be non-thrombogenic and non-hemolytic [6]. Since blood-material contact involves complicated mechanisms, it is not possible to predict the blood compatibility by considering the definitions given above. Even though the polymer or any other type of material fulfills the requirements described by some definitions, the blood response to the material should be evaluated for each specific of a material application. In many cases, it has been observed that 'so-called' blood compatible material would need further improvements for real life applications. The solution to the problem mainly requires modulating the physical and chemical properties of the material by modification or finding bioinert materials with respect to blood reactions [7].

The modification may be bulk modification or surface modification. Surface modification involves incorporation of hemocompatible chemical functionalities on the surface of the material without affecting the bulk properties considerably [8]. Poly (ethylene glycol) (PEG) [9], or zwitterionic molecules [10, 11, 12], heparin [13, 14], are examples to hemocompatible moieties. Bulk modification, is achieved by chemical grafting [15], physical mixing [16, 17] and copolymerization [18].

1.1.1.2 Host Response to Materials

Physicochemical properties of the material determined by its chemical composition, structure, morphology, crystallinity, porosity, surface charge and surface energy may affect the blood compatibility of a given material [19]. blood-material contact induces a series of immediate host responses. The mechanism involves neutrophils and macrophages activation, protein adsorption, activation of clotting cascade, platelets adhesion, and complement activation. Cytotoxicity and antibody production may also occur. Hypersensitivity, mutagenicity and reproductive toxicity or tumors formation are other possible adverse effects [19]. If a blood contact device or material is to be classified as hemocompatible these effects should be absent or at negligible level [20].

1.1.1.3 Protein Adsorption onto Biomaterials

When a material becomes in contact with blood, non-specific protein adsorption to the surface is triggered [21,22]. This process involves three steps: electrostatic attractions, hydrogen bonding or hydrophobic interactions; displacement of adsorbed proteins by others; and irreversible changes in protein conformation [3]. The adsorbed protein layer is identified by active receptors from platelets causing platelet adhesion and activation. This is followed by thrombus formation [23]. Fibrinogen has been identified as one of the main proteins that bind on the material surface in contact with blood [24, 25].

1.1.1.4 Cell – Biomaterial Interactions

In addition to the interactions between biomaterial and proteins, inflammatory responses are also induced during blood-material contact [26]. This response is characterized by neutrophils replaced by monocytes that differentiate into

macrophages that are cells with very long life time measured in terms of months [23].

1.1.1.5 Hemocompatibility Tests

General overview of the blood compatibility assessment evaluated by a series of proper tests is given in figure 1. Full blood compatibility assessment contains analysis of activation of the complement system, and hematologic evaluations to find out if there was hemolysis and leucocyte activation or any change in leucocyte numbers. Any changes in the platelet count, any adhesion of or any aggregation of platelets has to be determined. Platelet activation analysis and platelet function analyses are also included in the blood compatibility tests. Furthermore, any blood coagulation or induced thrombosis has to be characterized. Prothrombin time (PT) test measures extrinsic and common pathway of coagulation cascade activation. Measuring the ,Activated Partial Thromboplastin Time, (APTT) provide information about the activation of intrinsic and common coagulation pathway. Thrombin time (TT) is an indicator of the thrombin activity or fibrin polymerization [27].

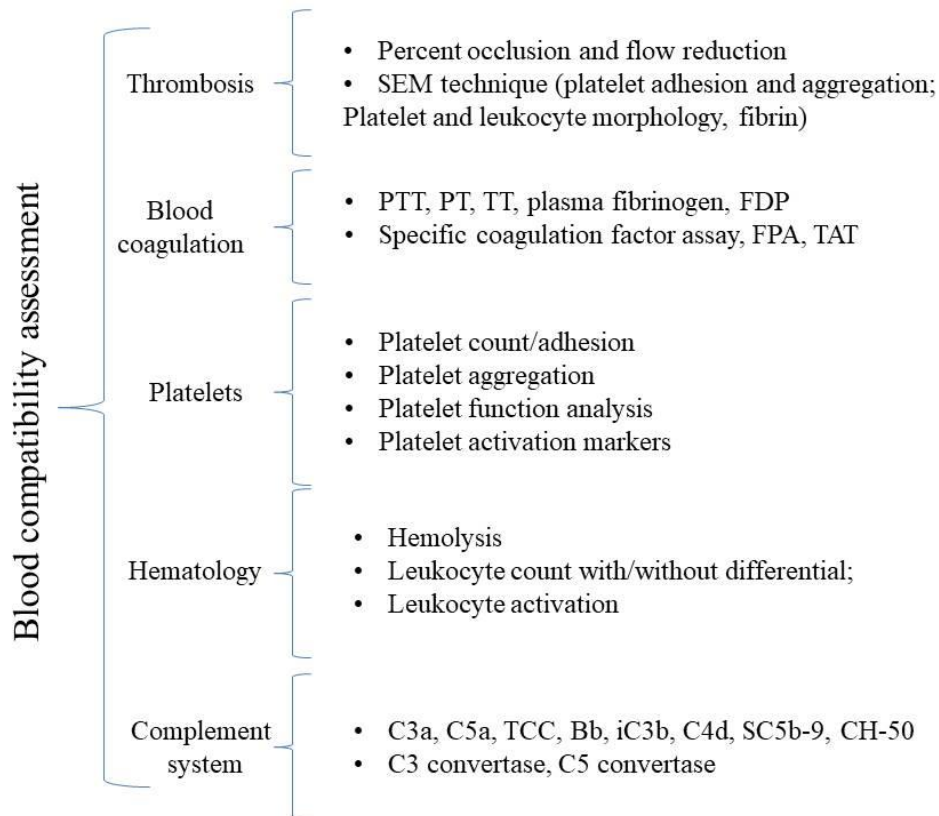


Figure 1: Blood compatibility assessment (adapted from ISO-10993-4:2002(E)).

1.2 Polymers as Biomedical Materials

Polymers can be applied as biomedical materials in various ways [28]. For example, they have found uses as drug delivery and gene delivery devices, as scaffolds in tissue engineering, as antimicrobial agents, as biosensors or agents in medical imaging. Polymeric hydrogels, which are usually biocompatible and often biodegradable, are often used for such applications. Radical polymerization accompanied by chemical crosslinking is the most common method used to prepare polymeric hydrogels. Physically crosslinked hydrogels are formed by establishing physical entanglements or physical interactions such hydrogen bonding or electrostatic interactions, or van der Waals interactions or hydrophobic interactions between the polymer chains.

Not only synthetic polymers but also natural polymers can be formed into hydrogels to act as biomaterials. They are obtained from plants and animals sources (Figure 2). Some examples are proteins, starch, cellulose, chitin, alginic acid. Main advantages of natural polymers over the synthetic ones are: they are environmentally friendly, nontoxic and biodegradable. They also show high biocompatibility.

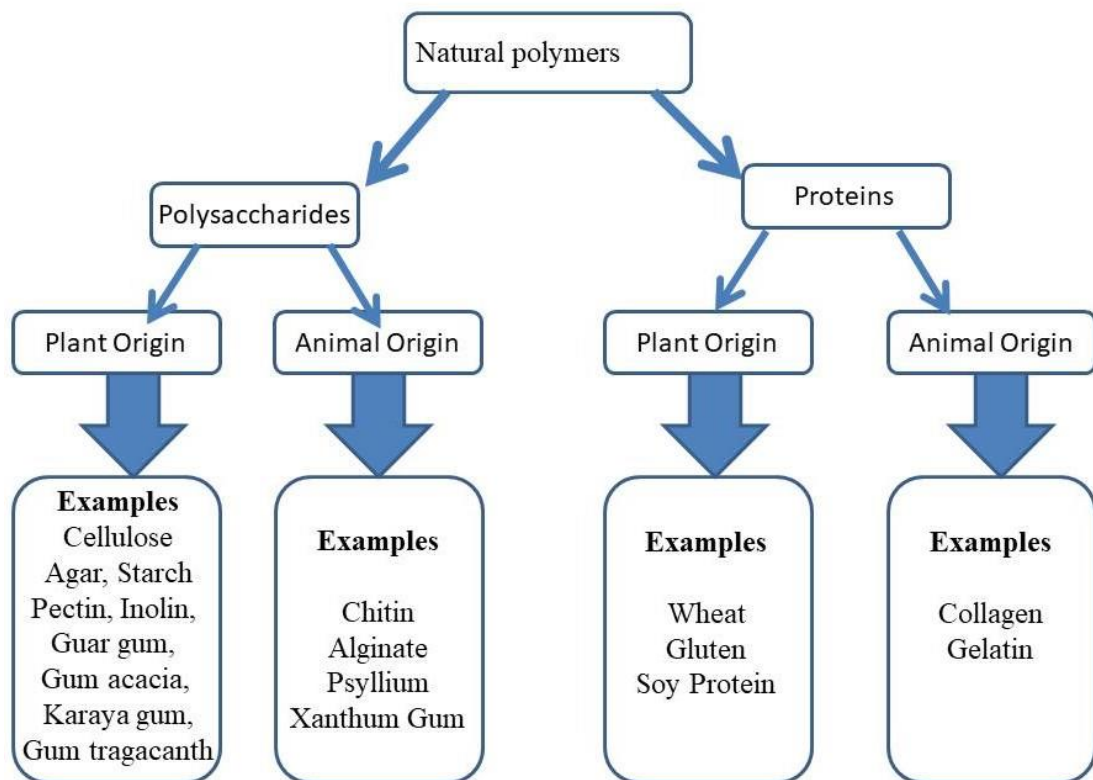


Figure 2: Classification of natural polymers

1.3 Grafting: Polymer Modification for Biomedical Applications

Applications of polymers as biomedical materials usually require modifications on the surface or bulk properties of the polymers. It is possible to modify polymer properties including wettability, permeability, biostability and/or chemical inertness, adhesion, biocompatibility, topography, surface charge and optical and frictional

properties by using chemical methods [29,30]. Grafting is a versatile method used to obtain modified polymer structures.

For example, acrylic acid has been grafted to polymer surfaces to form surface carboxylic acids [31]. Poly(ethylenimine), poly(allylamine), and chitosan have been bound to surface aldehydes or carboxylic acids to increase functionality in the form of primary amines [32]. By using such a polyfunctional agent, one can increase the number of reactive sites available on a surface for immobilization of bioactive compounds. For example, grafting poly(ethylenimine) to a surface onto which PEG is attached results in a high PEG density resulting in reduced protein adhesion [33].

1.3.1 Graft Copolymerization

Graft copolymers can be mainly made by three methods: (a) “grafting from”, method by which the polymerization of second monomer is initiated by sites placed on the main polymer chain; (b) “grafting onto” method where the polymeric species reacts with functional groups located on the another polymer chain; and (c) “grafting through” method in which the macro monomer is copolymerized with a small molecule comonomer.

Graft copolymers are made up of a backbone polymer chain to which one or more side chains (the branches) are chemically bonded through covalent bonds. The backbone and the branches could be homopolymers or copolymers, but they differ in composition or chemical nature. The branches may or not may not have equal lengths and random distribution over the backbone depending on the specific synthetic techniques used for their preparation. However, recent methods have allowed the synthesis of regular graft copolymers with equally spaced and identical

branches and of exact graft copolymers, where all the structural and molecular parameters can be accurately under control [34].

1.3.2 Optimization of Grafting Parameters

Grafting parameters such as grafting yield (%*G*), homopolymer yield (%*H*), and grafting efficiency (%*E*) were determined as follows:

$$\%G = \frac{W_2 - W_1}{W_1} \times 100 \quad (1)$$

$$\%H = \frac{W_4 - W_2}{W_3} \times 100 \quad (2)$$

$$\%E = \frac{W_2 - W_1}{W_3} \times 100 \quad (3)$$

Where, *w*₁, *w*₂, *w*₃, and *w*₄ denote the weight of initial polymer (the substrate), grafted polymer after extraction of any homopolymer formed, the monomer, and grafted polymer together with the homopolymer respectively [35].

These values are optimized with respect to the initiator concentration, temperature, time, and monomer concentration. Furthermore, the effect of any crosslinker, if present and the effect of other reaction conditions such as pH may need to be investigated.

1.4 Chitosan

Chitosan, a copolymer of β -(1 \rightarrow 4)-2-acetamido-2-deoxy-D-glucopyranose and β -(1 \rightarrow 4)-2-amino-2-deoxy-D-glucopyranose units has long been identified as a polymer with high biocompatibility, biodegradability, non-toxicity, antibacterial, antifungal activity, and muco-adhesion ability [37]. It is commercially made from N-deacetylation of chitin. Chitosan is a basic carbohydrate bearing free amine group as shown in Figure 3. Regarding the chemical structure shown in Figure 3, a variety of functional groups, namely the alcohol (-OH), amine (-NH₂) and acetamide

(NHC(O)) are present on chitosan backbone. Chitosan is a semicrystalline polymer in the solid state. A three dimensional network is formed through intermolecular H-bonding and hydrophobic Van der Waals interactions. The three-dimensional structure limits the solubility of chitosan in many solvents. In acidic media where the ionic strength is sufficiently high, solubility of chitosan is achieved. In the solid state, the temperatures of melting and glass transition of chitosan are higher than its temperature of thermal decomposition starting from 180 °C. As a result, except for the native forms, both gel and solid state of chitosan are formed from solution.

Solutions of chitosan represent the most important physical state of chitosan since many applications involve chitosan in solution, or useful other forms like fibers, gels, micro and nano particles, films are formed obtained from solution. Solution behavior of chitosan provides information on the role of structural parameters like degree of deacetylation (DD) and molecular weight distribution on the physical properties of the polymer. The origin and quality of the polymer also directly affect the properties.

Both covalent and physical gels of chitosan can be formed that may find applications in drug delivery, tissue engineering, and as bioadsorbents. Thermoreversible gels under some circumstances were obtained [37].

The free amine groups on chitosan provide the polymer with some important biological properties like mucoadhesivity. It also bears antitumor and wound healing activity as well as high adsorption capability.

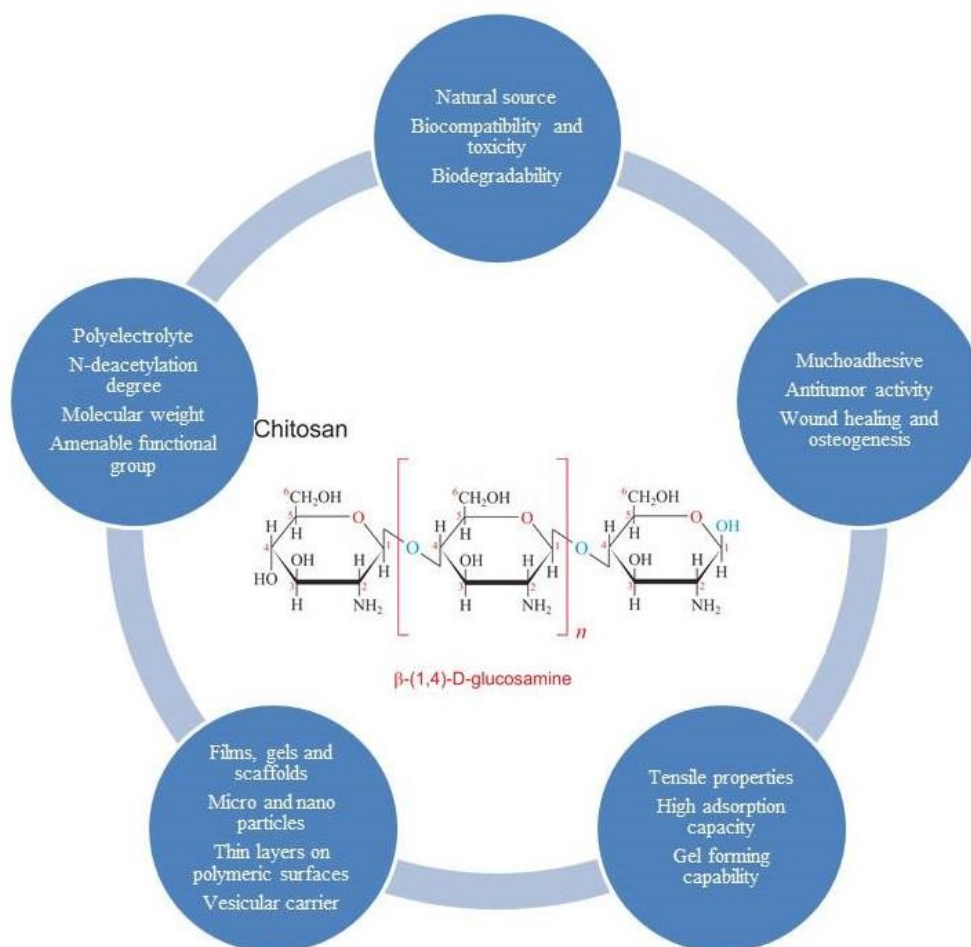


Figure 3: Chemical structure and main characteristics of chitosan

1.4.1 Blood Compatibility of Chitosan and Chitosan Derivatives

Hemocompatibility is one vital requirement for blood contacting materials. Blood is a complex entity, which is broadly made up of plasma, erythrocytes, and leukocytes and platelets. When it is brought into contact with a foreign material, adverse interactions may occur between blood and the material that may lead to activation and destruction of blood components. The general mechanism of blood-biomaterial interactions can be outlined as initial adsorption of a protein layer on the material surface, activation of the coagulation pathway, activation of leukocytes, adhesion and activation of platelets followed by thrombus formation [38]. Chitosan and its derivatives have been reported as promising hemostatic materials in various studies.

Even though the exact mechanism of hemostatic activity of chitosan is not very well known, increasing amount of data on the blood compatibility of chitosan and its derivatives in various forms such films, sponges, particles and fibers, allows more detailed analyses to be proposed on the blood coagulation activity of chitosan [39]. The cationic nature of chitosan is believed to induce thrombogenesis, which is an adverse biological response in blood contact applications. Two strategies have been employed to improve the hemocompatibility of chitosan. One is chemical modification, and the other one is incorporation of blood compatible compounds into the chitosan matrix [40]. Hemocompatibility studies on chitosan and chitosan derivatives by several different researchers have produced various results, which induce a need for further detailed analyses. For example, Malette et al [41] found that chitosan in acetic acid solution caused blood coagulation even in the presence of a blood thinner agent. A study by Klokkevold et al. [42] reported that chitosan in acetic acid solution stopped bleeding in rabbits. Another study reports that chitosan enhances platelet adhesion [43]. Biotinylated chitosan magnetic particles were found not to inhibit the prothrombin activity [44]. Carboxypropionylated chitosans, on the other hand, gave prolonged partial thromboplastin times [45]. Phosphorylcholine modified chitosan demonstrated to have improved protein anti adhesion ability and better hemocompatibility [46]. Ascorbyl chitosans have poorer hemocompatibility than chitosan, and give increased prothrombin times upon contact with human blood, *in vitro* [47].

1.4.2 Chitosan: Fe³⁺ Adsorbent for Biomedical Applications

Chitosan and chitosan derivatives are capable of forming complexes with metal ions [48]. Chitosan is well known to chelate metal ions in the following order: Cr³⁺ _Co²⁺ _Pb²⁺ _Mn²⁺ _Cd²⁺ _Ag¹⁺ _Ni²⁺ _Fe³⁺ _Cu²⁺ _Hg²⁺. The interaction between

chitosan and the metal ions occur by coordination via free electron pairs of nitrogen and oxygen atoms on chitosan backbone. It was proposed that the chitosan- iron complex formed by adsorption of iron onto chitosan is either hexa or penta - coordinated Fe(III). It was found that, for each Fe^{3+} ion, there are 4 moles of oxygen atoms and 2 moles of amino groups from two different chitosan chains. Also, at least one water molecule takes part in the coordination complex [49]. The adsorption studies carried out on chitosan and its derivatives show that amino groups are important binding sites over the chitosan backbone. In general adsorption isotherms obey Langmuir and Freundlich equations [50]. It is reported that the pH of the medium, concentration of the ions, and size of the chitosan particles all play role in the adsorption process [51]. The physicochemical parameters affecting the capability of chitosan to adsorb iron are degree of deacetylation, pH of the medium and concentration of the ferric ions [52].

Patients who suffer Thalassemia have to undergo frequent blood transfusions which lead to Fe^{3+} overload in their blood, Preliminary *in vitro* results from human blood serum indicate that chitosan is able to adsorb iron(III) in the body fluid medium and might be a suitable iron(III)-adsorbing agent in biological systems [52].

1.5 Poly (N-hydroxy ethyl acrylamide)

A number of antifouling polymers have common properties, such as being hydrophilic, electrically neutral, and hydrogen bond receptors but not hydrogen bond donors [53]. Poly (*N*-hydroxyethyl acrylamide) (PHEAA) is a nonionic, hydrophilic polymer with hydroxyl groups on the side chain that covers a hydrophobic carbon-carbon backbone shown in Figure 4. It is less adhesive to proteins than polyacrylamide (PAA).

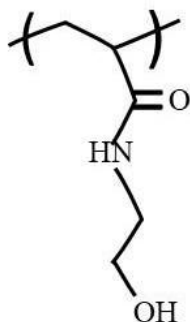


Figure 4: Poly (N-hydroxy ethyl acrylamide)

1.5.1 Biomedical Properties of the Homopolymer and Copolymers of HEAA

Poly (N-hydroxy ethyl acrylamide), polyHEAA, has been characterized as an antifouling polymer with low protein, bacteria and cell adherence. Poly (N-hydroxy ethyl acrylamide) brushes grafted on gold surfaces and gold nanoparticles proved to successfully repel nonspecific protein and bacteria adsorption on the substrates [54]. In another study, poly (N-hydroxy ethyl acrylamide)/salicylic acid hydrogels cross-linked with methylene bis acrylamide were shown to exhibit protein repellent and antibacterial activities [55]. Polymer brushes of carboxybetaine acrylamide and N-(2-hydroxy propyl methacrylamide) grown on gold surfaces demonstrated excellent antifouling activity in blood plasma and eggs [56].

1.6 Aims and Scope of the Thesis

A blood compatible polymer should be hydrophilic, electrically neutral, and should possess hydrogen bond acceptor sites. Furthermore, it should be non-thrombogenic and non-hemolytic. Poly (N-hydroxyethyl acrylamide) possesses all of these primary characteristics required for hemocompatibility. The hydroxyl substituent groups provide hydrophilicity and electrical neutrality, and act as hydrogen bond acceptor site together with the acrylamide group. Therefore, it is a candidate polymer to dilute the cationic nature of chitosan via chemical grafting without suppressing its

other powerful physical properties such as its film and gel forming properties. Since chitosan is known for its biocompatibility and polyHEAA for its protein, cell and bacteria antifouling properties the hybrid material has got the potential to improve the surface and bulk properties of chitosan as a biomaterial. As synthesis of chitosan-*graft*-polyHEAA copolymers have not been reported in the literature before, this study aims at finding out whether grafting is a suitable chemical process to incorporate poly (N-hydroxyethyl) chains onto chitosan backbone, if so, to identify the optimum process conditions, and to characterize the physicochemical characteristics of the products. Even though antifouling properties of polyHEAA and its copolymers have been studied thoroughly, its potential to contribute to hemocompatibility of polymer systems has not been reported before. In this thesis, blood contact properties of chitosan-*graft*-polyHEAA polymers have been investigated with respect to activated prothrombin time (PT) activated partial thromboplastin time (APTT), and platelet adhesion. Furthermore, glutaraldehyde crosslinked chitosan-*graft*-polyHEAA films were prepared and their iron(III) adsorption behaviour was investigated.

Chapter 2

EXPERIMENTAL

2.1 Materials

Following materials, instruments and methods were used to prepare and characterize the samples;

Chitosan medium molecular weight (450 kDa) with degree of deacetylation of 85% (Sigma-Aldrich) was used. Hydroxyethyl acrylamide (HEAA) (Sigma-Aldrich), potassium persulfate (KPS) (EDH Chemicals LTD), N,-N'-methylenebis(acrylamide) (MBA) (Titrachem), acetic acid (Sigma-Aldrich), acetone (Tekkim Kimya San), ethanol (Selim ve Oglu Ltd), hydrochloric acid (Merck), potassium chloride (Sigma-Aldrich), glutaraldehyde (Sigma-Aldrich), Iron (III) chloride (Sigma-Aldrich) were used as obtained without any further purification.

2.2 Equipment

The samples were prepared were characterized by FTIR (Percin Elmer spectrometer), UV-VIS Spectrophotometer (Percin Elmer, Spectrum Two spectrophotometer), XRD (Explorer, GNR, Italy) and SEM (LEO 1450 VP Scanning Electron Microscope) analyses. XRD, SEM and elemental analysis were carried out in Ferdowsi University, Mashhad, Iran.

2.3 Method

2.3.1 Grafting of Poly(N-hydroxyethyl acrylamide) onto Chitosan under Homogeneous Conditions

Chitosan (0.25 g) was dissolved in 25 mL of 1% v/v acetic acid solution, to give a 1% w/v polymer solution. Then, hydroxyethyl acrylamide (HEAA), and potassium per sulfate (KPS) were dissolved in the solution. Purging nitrogen gas through the system created an inert atmosphere. The reaction was carried out under nitrogen atmosphere at different temperatures and at different time intervals. The product was precipitated in acetone/ethanol mixture 50:50 and filtered. The solid residue was washed with distilled water and then treated with ethanol by soxhlet extraction to remove any homopolymer formed, or any unreacted monomer. The product was dried in the oven at 60°C to constant weight, and the dry mass was obtained to calculate the grafting percentage according to equation (1).

The reaction conditions and the grafting yields obtained are shown in Table 1. The samples soluble in aqueous media before drying became insoluble after drying due to thermal cross-linking.

Table 1: Synthesis of chitosan-*graft*-polyHEAA in aqueous solution

Sample	Optimization Factor	Chitosan (g)	HEAA (mL)	KPS (g)	MBA (g)	Time (h)	Temp (°C)
S1	Time	0.25	0.3	0.125	-	1	60
S2		0.25	0.3	0.125	-	3	60
S3		0.25	0.3	0.125	-	6	60
S4	HEAA	0.25	0.3	0.125	-	3	60
S5		0.25	0.6	0.125	-	3	60
S6		0.25	0.9	0.125	-	3	60
S7		0.25	1.2	0.125	-	3	60
S8		0.25	1.5	0.125	-	3	60
S9	KPS	0.25	0.9	0.050	-	3	60
S10		0.25	0.9	0.125	-	3	60
S11		0.25	0.9	0.250	-	3	60
S12	Temperature	0.25	0.9	0.05	-	3	50
S13		0.25	0.9	0.05	-	3	60
S14		0.25	0.9	0.05	-	3	70
S15	MBA	0.25	1.5	0.125	0.3	3	60
S16		0.25	-	0.125	0.3	3	60

2.3.2 Preparation of Films for Blood Compatibility Tests

A given amount of HEAA and/or MBA was dissolved in 15 mL of chitosan solution (1% w/v solution in 1% v/v acetic acid solution) in the presence of 0.075 g KPS at room temperature, as shown in Table 2. The mixture was then poured into a Petri dish, and the product was obtained as a film after solvent evaporation at 60°C for 72 h. The films were cleaned from impurities by first soaking in water, and then in 50:50 acetone/ethanol mixture. The MBA cross-linked products are named as chitosan-*graft*-(polyHEAA;MBA) or chitosan-*graft*-MBA, and the polyHEAA grafted products are named as chitosan-*graft*-polyHEAA.

A blank chitosan film (FBC) was obtained under similar experimental conditions, in the absence of the monomer, the initiator and the chemical cross-linker. All films were thermally cross-linked, and were insoluble in aqueous media after the cleaning procedures.

Table 2: Synthesis of chitosan-*graft*-polyHEAA and chitosan-*graft* (polyHEAA;MBA) Films*

Sample	HEAA(mL)	MBA (g)
F1	0.3	0.06
F2	0.6	0.06
F3	0.9	0.06
F4	-	0.06
F5	0.3	0.18
F6	0.6	0.18
F7	0.9	0.18
F8	-	0.18
F9	0.3	-
F10	0.6	-
F11	0.9	-
F12	Chitosan	

*(15 mL of 1% v/v acetic solution, 0.15 g chitosan, 0.075 g KPS, 60°C, 72 h)

2.3.3 Synthesis of Chitosan-*graft*-(polyHEAA; GA) Films

Samples were prepared based on 15 mL chitosan and filled in a beaker where KPS was added and nitrogen gas was purged, Then monomer (0.3 and 0.9)mL were added to each (as magnet was stirring) under mild temperature and after a quarter, crosslinker (0.1 and 0.3 mL) was added to their corresponding solutions and for a 15 more minutes they stirred well together to have homogeneous solution, meanwhile nitrogen was purged again (to the balloon with a loose parafilm seal) then were pasted as a tiny bed in small plastic made Petridis.

Finally, samples were placed in oven (40, 50 and 60°C) and a bit more nitrogen is purged in oven where thermal crosslinking is still ongoing gently. after 48 hours, the samples were ready. They were removed from the oven and placed in water bath

with dishes for a short time to tackle the hydrophobic properties of very dry sample. At the end when sample wets in bath, they were submerged in water to be washed (time to time water was refreshed) and finally were dried. Grafting percentage according to equation 1 was calculated.

Table 3: Synthesis of chitosan-graft-(PHEAA; GA) films characterization

Sample	HEAA monomer (mL)	GA (mL)	Product wt (g) 50°C
G1	0.3	0.1	0.49
G2	0.9	0.1	1.03
G3	-	0.1	0.21
G4	0.3	0.3	0.47
G5	0.9	0.3	1.10
G6	-	0.3	0.26
G7	0.3	-	0.41
G8	0.9	-	0.81
G9	Chitosan		0.15

2.3.4 Swelling Kinetics

Dry cross-linked sample films (0.05 g) were taken, immersed in water, removed from water at different time intervals and when leaking stopped the wet weight was recorded. Swelling percentage was calculated according to equation (4):

$$\% \text{ Swelling} = \frac{W_s - W_d}{W_d} \times 100 \quad (4)$$

Where w_s (g) and w_d (g) are the weights of swollen and dry hydrogels, respectively.

2.3.5 *In-vitro* Coagulation Test Analyses

The prothrombin time (PT) was measured using the blood plasma of healthy volunteers provided by Near East University Hospital, North Cyprus (Near East University Ethical Board Decision: 2017/49)(Appendix 1). Blood was filled into a liquid citrate loaded test tube. Citrate binds calcium and acts as an anticoagulant. Then the sample was centrifuged to isolate the plasma from the blood cells. Factor II (tissue factor) was added. The time that passes for blood clotting to occur was measured. International normalized ratio (INR) is a calculation made to normalize prothrombin time. INR is based on the ratio of the prothrombin time and the normal mean prothrombin time. The INR uses the ISI to equate all thromboplastins to the reference thromboplastin as given in equation (5).

$$INR = \left(\frac{patient\ PT}{Mean\ normal\ PT} \right)^{ISI} \quad (5)$$

Where ISI is international sensitivity index of the thromboplastin tested.

PT% is calculated as shown in equation (6):

$$PT\% = \frac{PT(control)}{PT(patient)} \times 100 \quad (6)$$

Partial prothrombin time (PTT) or activated partial thromboplastin time (APTT) was measured using STA compact hemostasis system equipment (Stage, US) for fresh human blood samples that were collected in citrate loaded tubes. The time was recorded up to the point of a clot formation. This test is called partial, as the reaction mixture is free of the tissue factor.

2.3.6 *In-vitro* Blood Contact Test

Samples were immersed into the fresh human whole blood from healthy donors for 30 minutes. Then the samples were washed with ultra pure water. The polymer films were then dried and examined under scanning electron microscope.

2.3.7 Human Serum Albumin (HSA) Adsorption

Polymer film samples (10 mg) were placed in 1.5 mL albumin (Albumin test kit, Human, Germany) solution of 1.0 mg/mL concentration at 37°C. Aliquots of 10 µL were taken at given time intervals and analyzed for albumin by photometry at 622 nm using bromocresol green. Each measurement was carried out in triplicate. Results were reported as the average of three measurements. HSA removal from solution was calculated using the initial and final absorbance values and a modified form of the relationship given in the prospectus of the albumin kit used (HUMAN-Germany) as shown in equation 7.

$$C_f = \frac{A_f}{A_i} \times C_i \quad (7)$$

A_f is final absorbance, A_i is initial absorbance and C_i is initial HSA concentration.

The amount of HSA adsorbed was calculated according to equation 8:

$$C_a = C_o - C_f$$

$$\%HSA \text{ removal} = \frac{C_a \times V_1}{W_1} \times 100\% \quad (8)$$

Where C_a stands for adsorbed HSA concentration (mg/L), C_o and C_f are the initial and final concentrations of HSA in ppm, V_1 is volume of solution (L), W_1 is weight of polymer in (g).

2.3.8 Fe^{3+} Adsorption on Chitosan-graft-(polyHEAA; GA) Films

0.01g polymeric samples were immersed in Fe^{3+} solution (4mL) in different concentrations, in a test tube. At different time intervals, 0.5 milliliter Fe^{3+} solution

from each test tube was taken and mixed with 0.5 milliliter of 5-sulfosalicylic acid dehydrate, (10% w/v), and completed to 4 milliliter with pH = 1 buffer solution. The absorbance of Fe³⁺ solution was recorded by visible spectrophotometry at $\lambda = 505$ nm using a Perkin Elmer spectrophotometer. Then the amount of Fe³⁺ ion adsorbed per gram sample was calculated according to equation 9.

$$\text{mg Fe}^{3+} \text{ adsorbed/g sample} = \left(\frac{C_o - C_f \times V_1}{W_1} \right) \left(\frac{Mw_2}{Mw_1} \right) \quad (9)$$

Where C_o and C_f are the initial and final concentrations of FeCl₃ in ppm, V₁ is volume of solution (L), W₁ is weight of polymer in (g), Mw₁ is molar mass for FeCl₃ (mg/mol) and Mw₂ is molar mass for Fe³⁺ (mg/mol).

Chapter 3

RESULTS AND DISCUSSION

3.1 Optimization of Grafting Parameters

Chitosan-*graft*-polyHEAA samples were synthesized in aqueous solution by persulfate. Figure 5 shows the optical images of the film and the powder forms of the samples obtained. The grafting parameters were optimized with respect to time, temperature, HEAA and KPS concentrations. Grafting yield (%G) values were calculated using gravimetric data. The values obtained are given in Table 4. When the effect of reaction time on the grafting yield is examined, we can see that the time does not have a profound effect on the grafting yield. The grafting yield is 140% at 1 h and 180% at 3 h. The value then decreases slightly to 164% at 6 h. Increasing the temperature from 50°C to 60°C, gives a product with a higher grafting yield. The value obtained at 50°C is 240%, while it is 380% at 60°C. A reaction temperature of 60°C yields lower %G (380%) value than at 70°C (420%). Similarly, higher amounts of KPS do not produce considerably higher %G values within the 0.05 g- 0.25 g range. The values are 380%, 420% and 460% for 0.05 g, 0.125 g and 0.25 g KPS in the reaction medium respectively. Increasing HEAA, on the other hand, results in higher grafting yields within 0.3 mL - 1.5 mL range studies in 25 mL 1% w/v chitosan solution indicating that once grafting is initiated chain growth occurs according the amount of the monomer available. Optimum conditions have been determined as 0.25 g chitosan, 1.5 mL HEAA, 0.125 g KPS in 25 mL aqueous solution at 60°C, and 3h reaction time under nitrogen atmosphere (S8). The highest

grafting yield was obtained as 640% under these conditions. All samples were soluble in aqueous solution when dried under the atmospheric condition. However, they underwent thermal cross-linking upon drying in the oven at 60°C. They were completely insoluble in aqueous media after 24 h drying in the oven at 60°C. An MBA cross-linked network graft copolymer was obtained by carrying out the grafting reaction under optimum conditions in the presence of 0.3 g MBA. A total %G value of 700% was recorded for the chitosan-*graft*-(polyHEAA;MBA) (S15) sample obtained. When the reaction was carried out in the absence of HEAA, only 87.9% grafting yield was obtained for the chitosan-*graft*-MBA sample (S16).

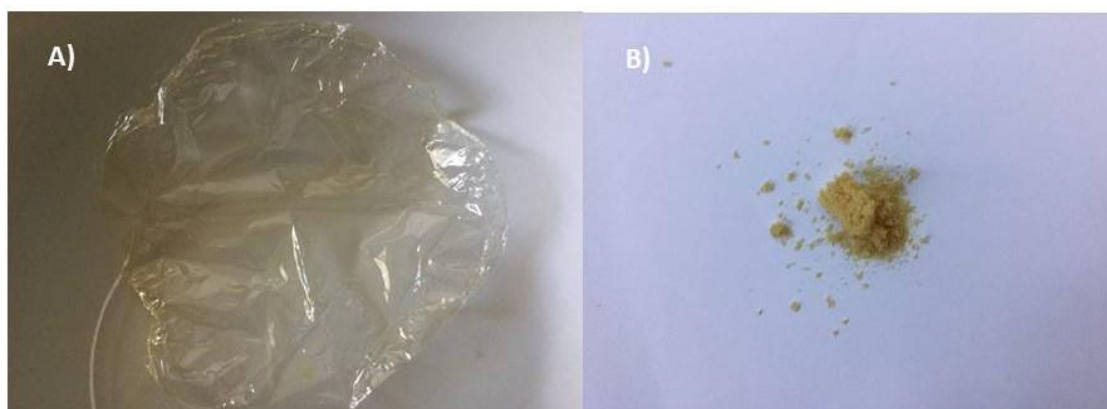


Figure 5: (A) chitosan-*graft*-(polyHEAA;MBA) film and (B) chitosan-*graft*-(polyHEAA;MBA) powder

Table 4: Synthesis of chitosan-*graft*-polyHEAA in aqueous solution

Sample	Optimization Factor	Chitosan (g)	HEAA (mL)	KPS (g)	MBA (g)	Time (h)	Temp (°C)	%G ± 10
S1	Time	0.25	0.3	0.125	-	1	60	140
S2		0.25	0.3	0.125	-	3	60	180
S3		0.25	0.3	0.125	-	6	60	164
S4	HEAA	0.25	0.3	0.125	-	3	60	180
S5		0.25	0.6	0.125	-	3	60	260
S6		0.25	0.9	0.125	-	3	60	420
S7		0.25	1.2	0.125	-	3	60	460
S8		0.25	1.5	0.125	-	3	60	640
S9	KPS	0.25	0.9	0.05	-	3	60	380
S10		0.25	0.9	0.125	-	3	60	420
S11		0.25	0.9	0.25	-	3	60	460
S12	Temperature	0.25	0.9	0.05	-	3	50	240
S13		0.25	0.9	0.05	-	3	60	380
S14		0.25	0.9	0.05	-	3	70	420
S15	MBA	0.25	1.5	0.125	0.3	3	60	700
S16		0.25	-	0.125	0.3	3	60	87.9

Experimental conditions and grafting yields for the film samples that were prepared for blood compatibility experiments are given in Table 5. When both MBA and HEAA are present in the sample %G value represents total grafting of both components. The grafting medium was set as 0.075 g KPS and a predetermined amount of HEAA and MBA dissolved in 15 mL 1% w/v chitosan solution. Films were obtained after solvent evaporation at 60°C for 72 h. Increasing grafting yield values with increasing amount of HEAA in the presence of either 0.06 g or 0.18 g MBA were obtained under the given conditions. In the presence of 0.06 g MBA, 0.3, 0.6 and 0.9 mL HEAA produced chitosan-*graft*-(polyHEAA;MBA) films with 146% (F1), 313% (F2) and 633% (F3) grafting yields respectively. Similar samples, F5, F6 and F7 obtained in the presence of 0.18 g MBA, gave 253%, 333% and 406% grafting yields respectively. In the absence of HEAA, samples F4 and F8 were found to have 33.3% and 86.6% grafting values, respectively. When grafting yields of the film samples F9, F10, F11 are considered, it can be followed from Table 5 that the values are almost independent of the amount of HEAA. We obtained film samples with 313%, 326% and 333% grafting yields for F9, F10 and F11, respectively. This behavior can be attributed to the formation of higher fraction of water-soluble homopolymer with a higher amount of HEAA in the absence of the chemical cross-linker, MBA. The water-soluble portion should leach out during the washing procedure from the thin film matrix, leaving behind a thermally cross-linked product with a given %G value.

Table 5: Synthesis of chitosan-*graft*-polyHEAA and chitosan-*graft*-
(polyHEAA;MBA) Films

Sample	HEAA (mL)	MBA (g)	%G
F1	0.3	0.06	146
F2	0.6	0.06	313
F3	0.9	0.06	633
F4	-	0.06	33.3
F5	0.3	0.18	253
F6	0.6	0.18	333
F7	0.9	0.18	406
F8	-	0.18	86.6
F9	0.3	-	313
F10	0.6	-	326
F11	0.9	-	333
F12		chitosan film	

3.1.1 FTIR Analysis

In the FTIR spectrum of chitosan shown in Figure 6A, a characteristic amide band at 1649 cm^{-1} , the C–H bending vibrations in the $1400\text{--}1500\text{ cm}^{-1}$ region, the –CH_3 bending at 1380 cm^{-1} , C–H stretching at 2884 and 2974 cm^{-1} and O–H stretching at 3339 cm^{-1} are observable. The hydroxyethyl acrylamide (HEAA) spectrum shown in Figure 6B exhibits all characteristic absorption bands of –C–C , –C=C– , C–H, C–O, and O–H. The spectrum of chitosan-*graft*-polyHEAA and chitosan-*graft*-(polyHEAA;MBA) is shown in Figure 6C and D respectively. The spectra exhibit amide carbonyl bands at $1643\text{--}1633\text{ cm}^{-1}$, and at $1549\text{--}1556\text{ cm}^{-1}$. These bands have been taken as evidence of grafting of HEAA or MBA onto chitosan. One representative structure proposed for the chitosan-*graft*-(polyHEAA;MBA) product is shown in Figure 7. The structure based on the reactivity of functional groups, FTIR data and previously proposed grafting and cross-linking mechanisms [72, 73].

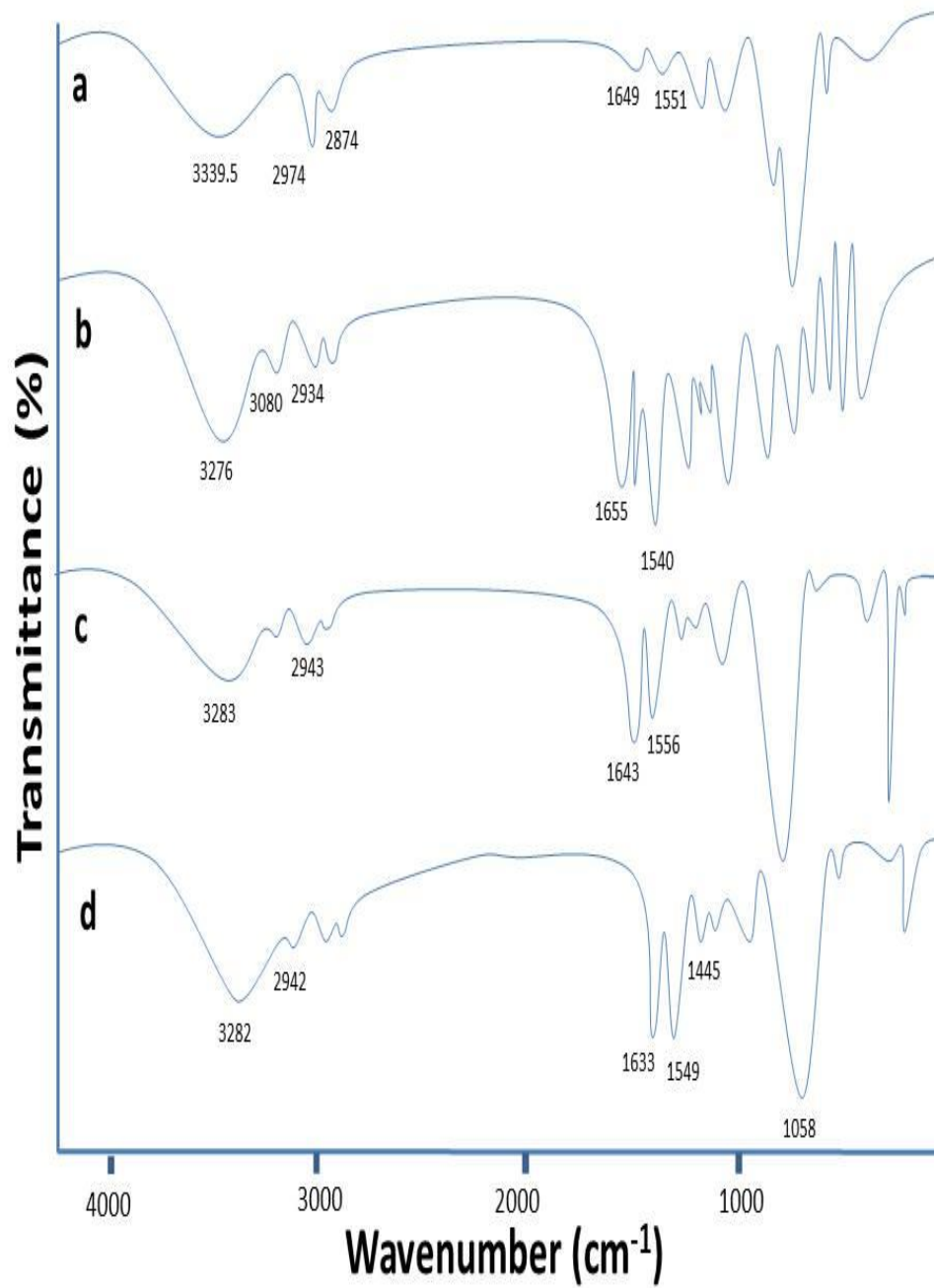


Figure 6: FTIR spectrum of a) chitosan, b) polyHEAA, c) chitosan-*graft*-polyHEAA (S8), d) chitosan-*graft*-(polyHEAA;MBA) (S15)

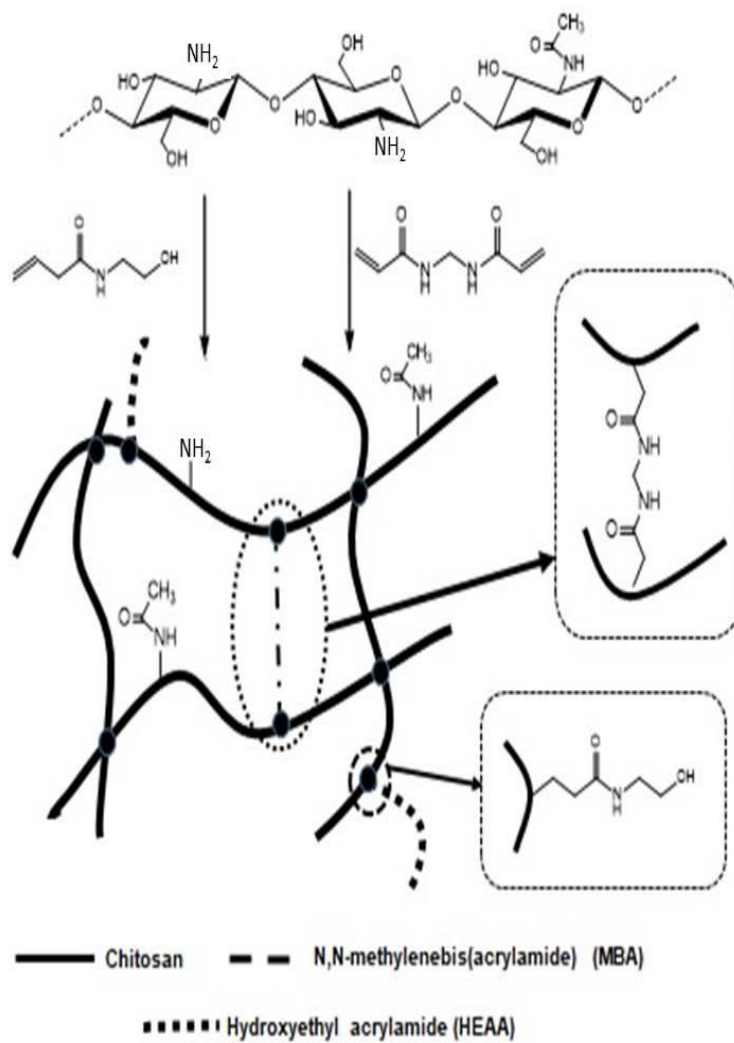


Figure 7: Proposed structure for chitosan-*graft*-(polyHEAA;MBA)

3.1.2 XRD Analysis

XRD patterns of film samples F7, F8, F9, F11 and F12 are given in Figure 8. The crystallinity index of each sample was calculated according to equation (10):

$$CrI = \frac{I_c - I_a}{I_c} \quad (10)$$

Where, I_c and I_a are intensities of the crystalline peak of chitosan at 20° and 8° respectively [81].

Chitosan sample (F12) bears the highest crystallinity index calculated as 0.75. Chitosan-*graft*-polyHEAA films (F9 and F11) have crystallinity indices of 0.55 and 0.50 respectively. Therefore, grafting reaction results in decrease in crystallinity of the polymer sample. Sample F7, chitosan-*graft*-(polyHEAA;MBA) shows a crystallinity index of 0.58. Since -OH and -NH₂ groups on the chitosan backbone are used up as the grafting sites, the spatial arrangement of functional groups on the polymer chain is disturbed, and hence the probability of intermolecular hydrogen bonding and orderly arrangement of the chitosan chains decreased. This phenomenon is reflected as a decrease in the crystallinity of the polymer. Similar observations have been reported with other grafted chitosans [78, 79]. Chitosan-*graft*-MBA sample (F8) is completely amorphous indicating a high degree of cross-linking leading to the loss of orderly arrangement of chitosan chains. A low equilibrium % swelling value for sample F8 compared to the other samples provides further evidence for a highly cross-linked sample.

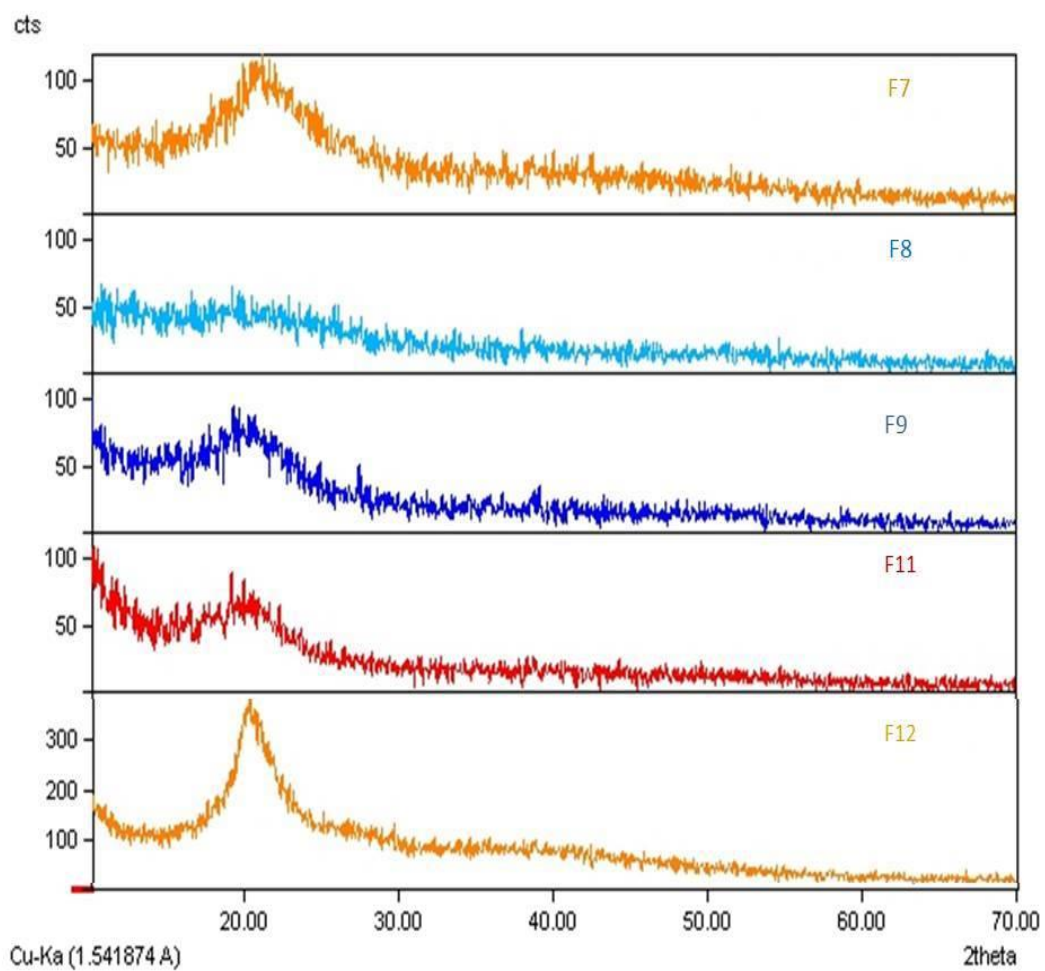


Figure 8: XRD pattern of F7: chitosan-*graft*-(polyHEAA;MBA) (%G=406), F8: chitosan-*graft*-MBA (%G=86.6%), F9: chitosan-*graft*-polyHEAA (%G=313%) F11: chitosan-*graft*-polyHEAA (%G=333%), F12: chitosan

3.1.3 SEM Analysis

The surface morphologies of grafted products were examined using SEM images as given in Figure 9. Surfaces of chitosan-*graft*-(polyHEAA;MBA) and chitosan-*graft*-MBA in powder form are compared to each other in Fig 9A and 9B, respectively. Both samples have rough surfaces due to the grafted chains on the chitosan backbone. Chitosan-*graft*-MBA bears a more porous surface (Figure 9B) while simultaneous grafting with polyHEAA chains fills in the pores to produce a more compact surface morphology (Figure 9A). SEM pictures of chitosan-*graft*-(polyHEAA;MBA), chitosan-*graft*-MBA, chitosan-*graft*-polyHEAA, and chitosan films are shown in Figure 9C, D, E, and F, respectively. When the surface morphologies of chitosan-*graft*-(polyHEAA;MBA) (Figure 9C) and chitosan-*graft*-MBA (Figure 9D) films are compared to each other, it can be observed that pores are available on the surface of chitosan-*graft*-MBA while the surface of chitosan-*graft*-(polyHEAA;MBA) is much more homogeneous lacking the pores present on chitosan-*graft*-MBA film similar to the pattern revealed by the corresponding samples in the powder form shown in Figure 9A and 9B. The pores on the chitosan-*graft*-MBA sample are due to the chemically cross-linked nature of the sample. As explained above, pores are filled by the grafted polyHEAA chains in chitosan-*graft*-(polyHEAA;MBA) sample. The surfaces of chitosan-*graft*-polyHEAA, Figure 9E, and chitosan (Figure 9F) are smooth due to the absence of any chemical cross-linking agent.

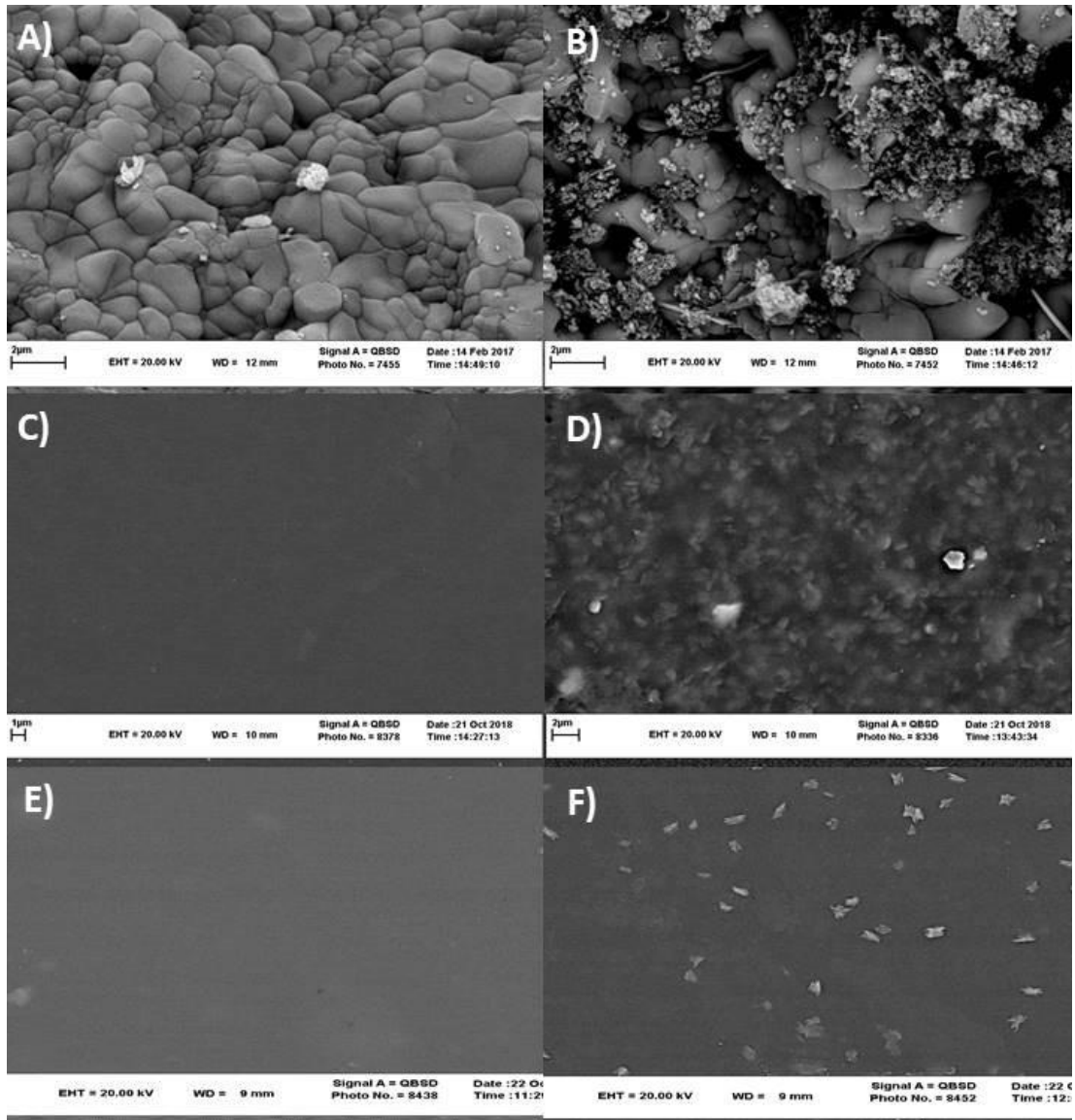


Figure 9: SEM picture of A) S15: chitosan-*graft*-(polyHEAA;MBA) powder, B) S16: chitosan-*graft*-MBA powder, C) F7: chitosan-*graft*-(polyHEAA;MBA), F8: chitosan-*graft*-MBA, F11: chitosan-*graft*-polyHEAA, and F12: chitosan (F12) film

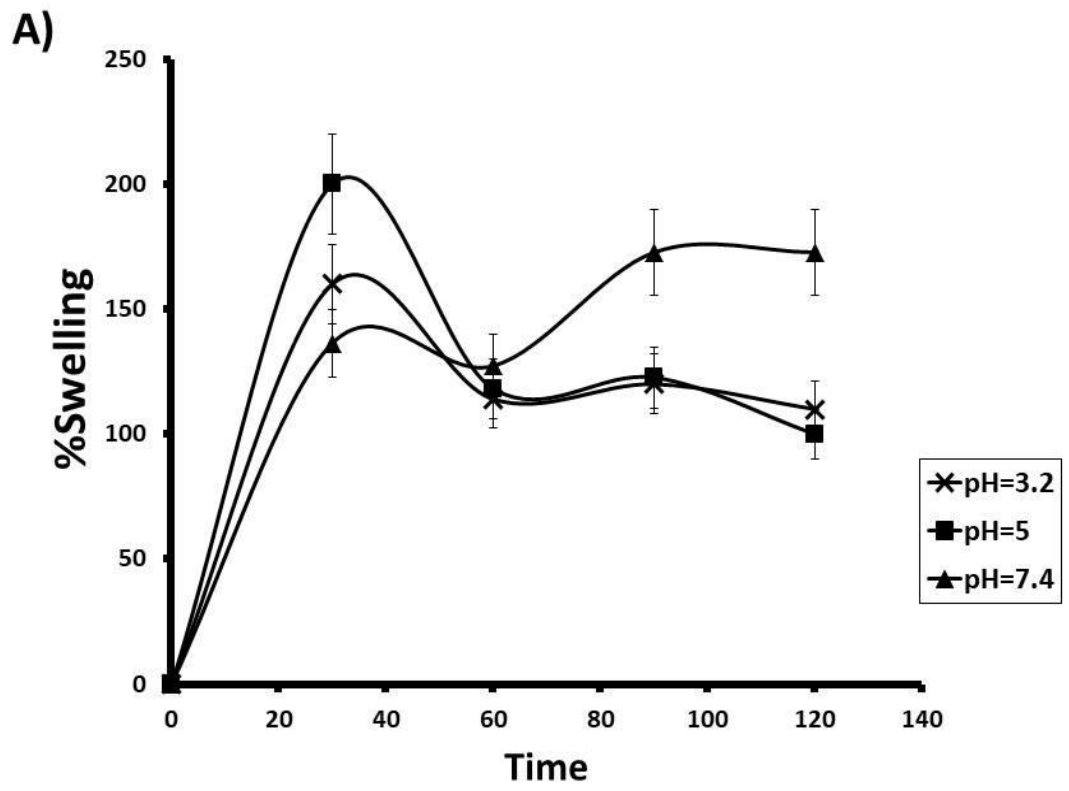
3.1.4 Swelling Behaviour of Chitosan-graft-polyHEAA and Chitosan-graft-(polyHEAA;MBA) Films

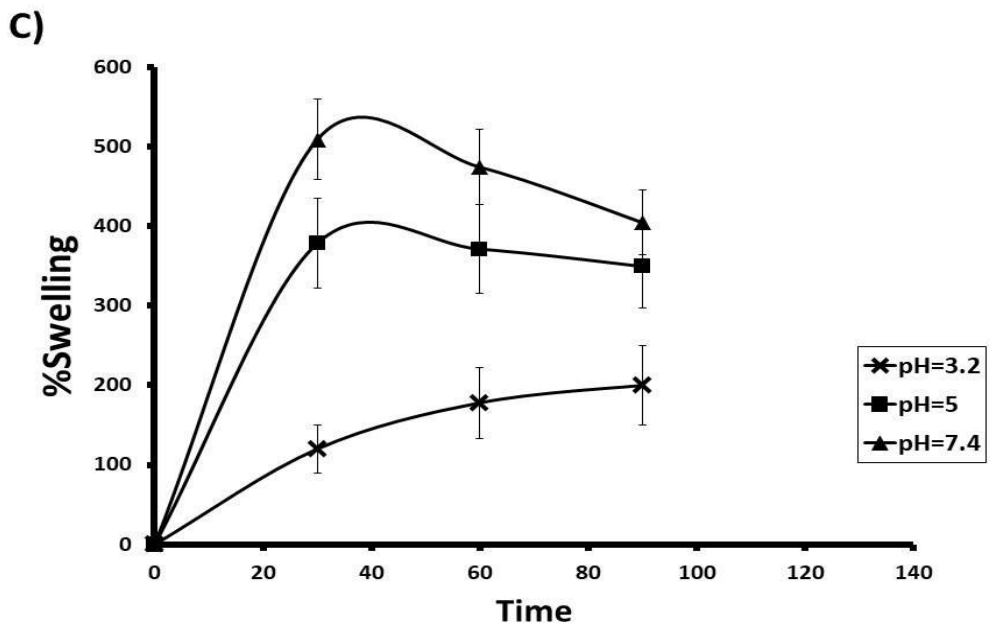
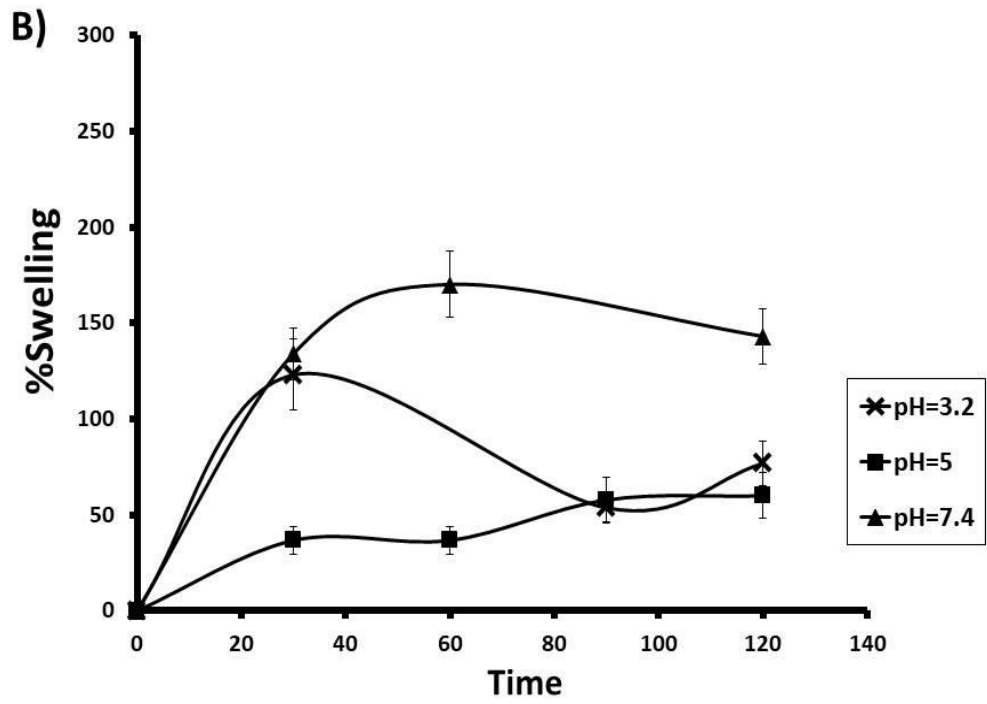
Swelling behaviour of chitosan-graft-(polyHEAA;MBA) (F7), chitosan-graft-MBA (F8), chitosan-graft-polyHEAA (F11), and chitosan (F12) films are illustrated in Figure 10A, B, C, and D and Table 6 (F7,8,11 and 12) at three different pH values of 3.2, 5.0 and 7.4 with average 10% error. All samples reach a maximum swelling degree, which reduces to the equilibrium % swelling value within a one hour contact with aqueous solution. The samples swell in acidic media due to the protonation of the amine groups present on the chitosan backbone. Swelling degrees of all samples are higher in aqueous solution with pH = 7.4 due to the partial hydrolysis of the acrylamide group to carboxylic acid and to carboxylate functionalities at moderately acidic and at neutral pH values. Thermally cross-linked chitosan-graft-polyHEAA (%G= 333), sample F11, exhibits the highest swelling capacity in aqueous solution. It bears an equilibrium % swelling capacity of 200%, 350% and 400% at a pH value of 3.2, 5.0 and 7.4, respectively. Sample F7, chitosan-graft-(polyHEAA;MBA) (%G=406) demonstrates a smaller swelling capacity than sample F11, due to the chemical cross-links formed by MBA molecules in between the chitosan polymer backbones. F7 swells to 110%, 100% and 173% in aqueous solutions of pH 3.2, 5.0 and 7.4. Chitosan-graft-MBA (%G=86.6), on the other hand, sample F8, swells less than both F7 and F11 with equilibrium swelling degrees of around 60% at pH 3.2 and pH 5 and 140% at pH 7.4. The film formed by the polymer chitosan; sample F12, swells to 150% at pH 7.4. Chitosan dissolves in acidic media due to the presence of amine functionality on the chain backbone. The results reveal that cross-linking chitosan via grafting by a difunctional monomer, MBA, causes a decrease in the swelling ability at pH 7.4. However, it imparts durability and swelling capability

under acidic conditions. Grafting polyHEAA onto chitosan whether cross-linked with MBA or not furnishes the polymer with a higher degree of hydrophilicity.

Table 6: Swelling behavior over time for F7: chitosan-*graft*-(polyHEAA;MBA) (%G=406), F8: chitosan-*graft*-MBA (%G=86.6%), F11: chitosan-*graft*-polyHEAA (%G=333%), F12: blank chitosan at pH 7.4

Sample	time	pH=3.2	pH=5	pH=7.4
F7	30	160	200	136.4
	60	114	118.2	127.3
	90	120	122.7	172.7
	120	110	100	172.7
F8	30	123.1	36.8	134.2
	60	-	36.8	170.3
	90	53.8	57.9	-
	120	76.9	60	143.2
F11	30	120	378.3	508.7
	60	178	371	473.9
	90	200	349.3	404.3
	120	-	-	-
F12	30	disintegrated		185.7
	60			219.3
	90			135.3
	120			135.3





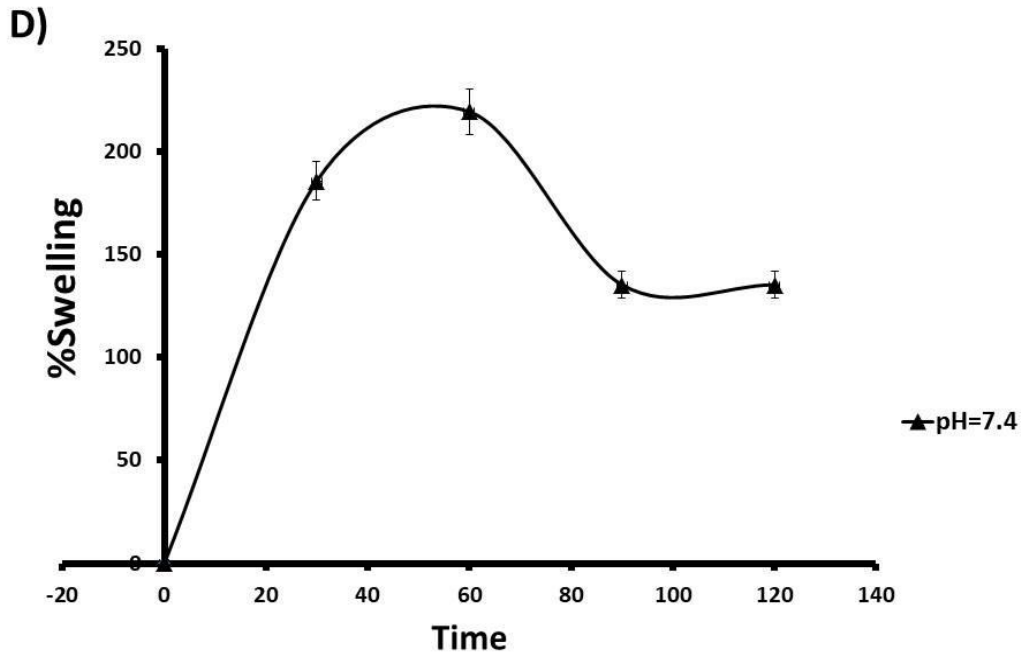


Figure 10: Swelling behavior over time for A) F7: chitosan-*graft*-(polyHEAA;MBA) (%G=406), B) F8: chitosan-*graft*-MBA (%G=86.6%), C) F11: chitosan-*graft*-polyHEAA (%G=333%), D) F12: chitosan at pH 7.4

3.1.5 *In vitro* Coagulation Test Analyses

As blood-material contact may induce several complex biochemical reactions such as activation of the complement system, and activation of the intrinsic and extrinsic pathways leading to blood clotting, it is useful to study prothrombin time (PT) and partial thromboplastin time (APTT) to obtain evidence with regard to the potential of the biomaterial as a blood-contacting device. Both PT and APTT measure the time taken for the blood to clot. PT together with international normalized ratio (INR) measures the extrinsic coagulation pathway. APTT works for the intrinsic coagulation and common coagulation pathways. PT and APTT are determined in the presence and in the absence of the tissue factor, respectively.

A preliminary evaluation of the compatibility of chitosan, chitosan-*graft*-polyHEAA, and chitosan-*graft*-(polyHEAA;MBA) films with human blood was carried out by

investigating their ability to alter the blood coagulation times, *in vitro*. PT, INR, PT % and APTT values were determined. The reference values are provided as 23.6-35.2 seconds for APTT, 11.5-15 seconds for PT, by the laboratory where the analyses were carried out. Reference INR value is provided as 0.8-1.2 and PT % as 70-120, by the same laboratory. It can be followed from Figure 11 A, B, C and D and Table 7 A, B, C and D that initial PT, INR, PT% and APTT values of each blood sample before contact with any given polymer film lie within normal ranges. After contact for 15 min with the polymer film, PT time for the blood sample in contact with chitosan (F12) increases to 21.1 s, and then shows a trend to fall in time but remains above limits (16.8 s) after 90 min blood-polymer contact. This value corresponds to a 32% increase in PT time after contact for 90 min. Chitosan-*graft*-MBA (F8) causes an increase in the PT time from 12.7 s to 19.7 s after 90 min contact, causing a 55% increase in the PT time. Samples F9, and F11, thermally cross-linked chitosan-*graft*-polyHEAA samples, on the other hand, produce very little changes in PT times, 3.9% and 0.7% respectively. However, chitosan-*graft*-(polyHEAA;MBA) sample (F7) causes a 37 % increase in the PT time. Hence, it can be concluded that chitosan film (F12), MBA cross-linked chitosan film (F8) and MBA cross-linked chitosan-*graft*-polyHEAA film (F7) induce anticoagulant activity upon contact with blood. Grafting chitosan with polyHEAA (F9 and F11), on the other hand, results in inert film surfaces with regard to blood clotting activity. These behaviors should be related to both chemical composition and to the physical characteristics of the solid polymer substrates. The physicochemical characteristics may enhance or reduce the anticoagulant activity of chitosan observed in this study. When data available from XRD and SEM analyses are considered together, we can see that chitosan film bearing a crystallinity crystallinity index of 0.75, and smooth,

non-porous surface triggers inhibition of blood clotting mechanisms. Previous study on anticoagulant activities of chitosan and ascorbyl chitosans revealed that calcium ion chelating ability of chitosan should play a role in its anticoagulant activity by blocking the function of vitamin K [15]. Furthermore, chitosan may interact with the acid groups on the cells providing a mechanism for disruption of the coagulation pathway [50]. Cross-linking with MBA (F8) results in an almost completely amorphous material with a porous surface designed by interwoven polymer chains as revealed by the SEM pictures (Fig 9). The amorphous and microporous nature of sample F8, should allow increased adsorption on the film surface of calcium or any other blood component triggering anticoagulant activity. Hence, this sample causes the longest PT and APTT times. Samples F9 and F11, with a smaller crystallinity degree of 0.55 and 0.50 respectively, and non-porous film surfaces are expected to act as better adsorbents than chitosan, and cause prolonged thrombin times. On the contrary, they do not cause any significant effect on the blood clotting times. This behavior is attributed to the hydrophilicity and antifouling effect of polyHEAA grafted onto chitosan. Sample F7, *chitosan-graft-(polyHEAA; MBA)* with crystallinity index of 0.58, exhibits medium blood anticoagulant properties better than chitosan but worse than *chitosan-graft-MBA*. While less crystallinity than chitosan provides better adsorptive capacity than chitosan that should increase anticoagulant activity, presence of polyHEAA grafted on the chains causes a counteraction. Even though blood coagulation times provide preliminary evidence on the anticoagulant activity or thrombogenicity of the biomaterial, further tests such as generation of activation factors in the blood plasma, changes in platelets, and blood cells, adhesion of platelets, cells and proteins on the material surface should be investigated to be able to classify the hemocompatibility of the material under study.

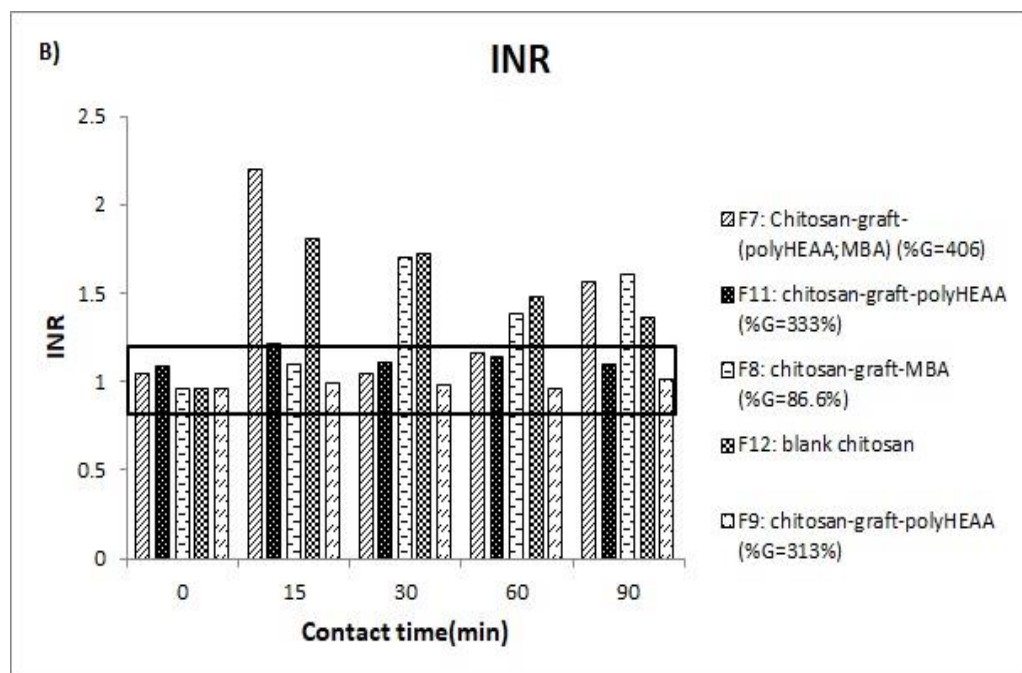
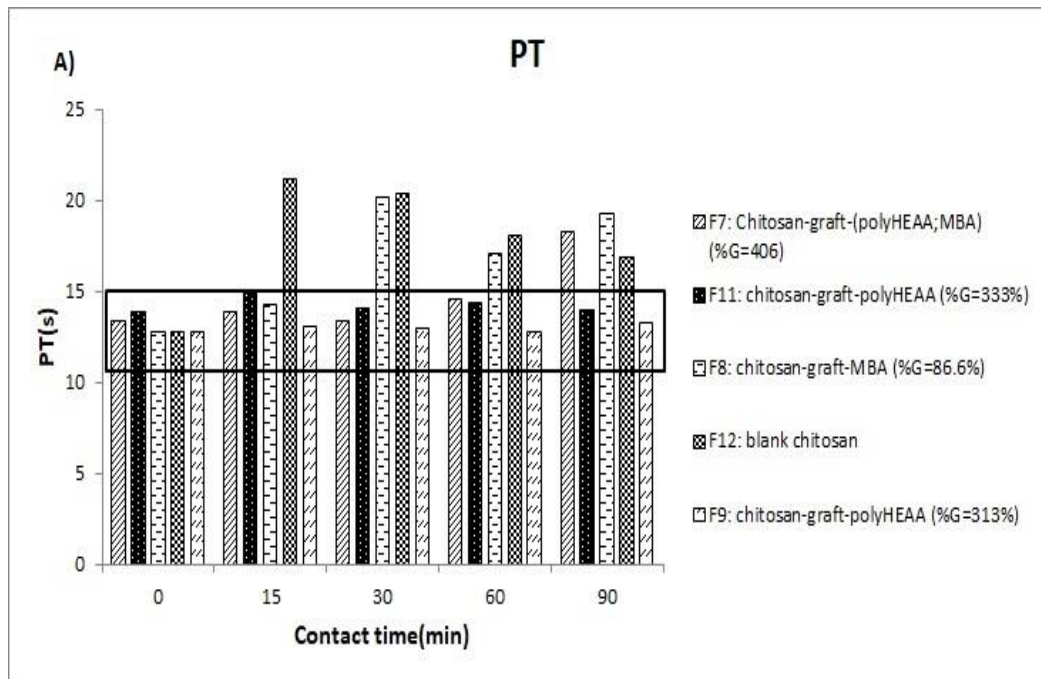
Table 7: A) prothrombin time B) international normalized ratio C) PT percent D) activated partial thromboplastin time for F7: chitosan-*graft*-(polyHEAA;MBA) (%G=406), F8: chitosan-*graft*-MBA (%G=86.6%), F9: chitosan-*graft*-polyHEAA (%G=313%) F11: chitosan-*graft*-polyHEAA (%G=333%), F12: chitosan

A)	0	15	30	60	90	Reference values
F7: Chitosan- <i>graft</i> -(polyHEAA;MBA) (%G=406)	13.3	13.8	13.3	14.5	18.2	
F8: chitosan- <i>graft</i> -MBA (%G=86.6%)	12.7	14.2	20.1	17	19.2	11.5-15
F9: chitosan- <i>graft</i> -polyHEAA (%G=313%)	12.7	13	12.9	12.7	13.2	
F11: chitosan- <i>graft</i> -polyHEAA (%G=333%)	13.8	14.9	14	14.3	13.9	
F12: blank chitosan	12.7	21.1	20.3	18	16.8	

B)	0	15	30	60	90	Reference values
F7: Chitosan- <i>graft</i> -(polyHEAA;MBA) (%G=406)	1.04	2.2	1.04	1.16	1.56	
F8: chitosan- <i>graft</i> -MBA (%G=86.6%)	0.96	1.1	1.7	1.38	1.61	
F9: chitosan- <i>graft</i> -polyHEAA (%G=313%)	0.96	0.99	0.98	0.96	1.01	0.8-1.2
F11: chitosan- <i>graft</i> -polyHEAA (%G=333%)	1.09	1.21	1.11	1.14	1.1	
F12: blank chitosan	0.96	1.81	1.72	1.48	1.36	

C)	0	15	30	60	90	Reference values
F7: Chitosan- <i>graft</i> - (polyHEAA;MBA) (%G=406)	93	35	93	78	52	
F8: chitosan- <i>graft</i> -MBA (%G=86.6%)	107	85	48	62	51	
F9: chitosan- <i>graft</i> -polyHEAA (%G=313%)	107	102	104	107	107	70-120
F11: chitosan- <i>graft</i> -polyHEAA (%G=333%)	86	74	84	80	86	
F12: blank chitosan	107	44	47	56	63	

D)	0	15	30	60	90	Reference values
F7: Chitosan- <i>graft</i> - (polyHEAA;MBA) (%G=406)	26.1	32.2	30.3	41.5	38.2	
F8: chitosan- <i>graft</i> -MBA (%G=86.6%)	28.6	35.1	43.2	32.5	37.3	
F9: chitosan- <i>graft</i> -polyHEAA (%G=313%)	28.6	38.1	30.4	28.8	34.1	23.6-35.2
F11: chitosan- <i>graft</i> -polyHEAA (%G=333%)	29.4	32	31.4	31.7	31.6	
F12: blank chitosan	28.6	56.7	53.1	43.5	40.5	



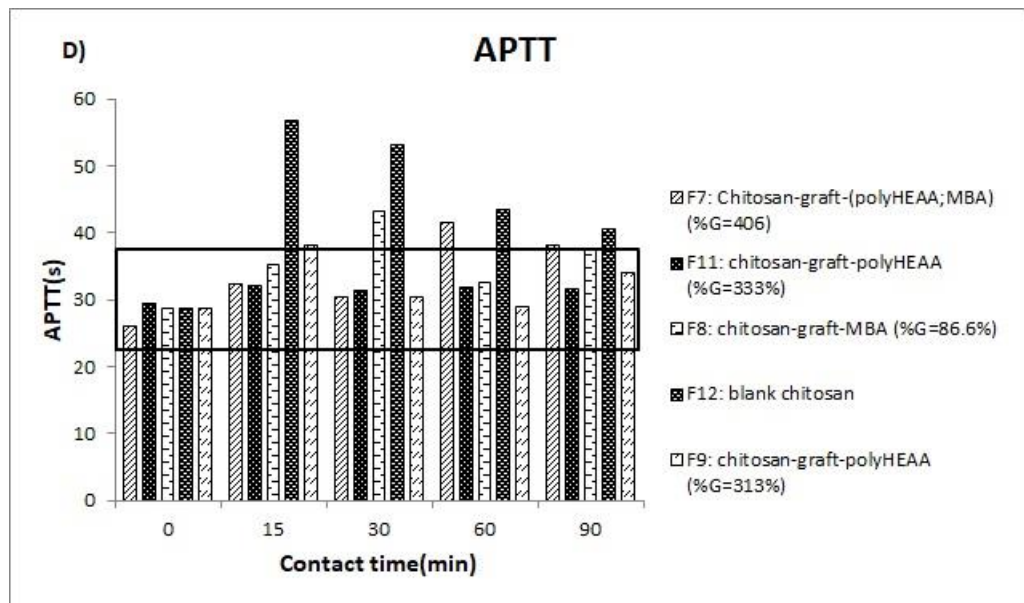
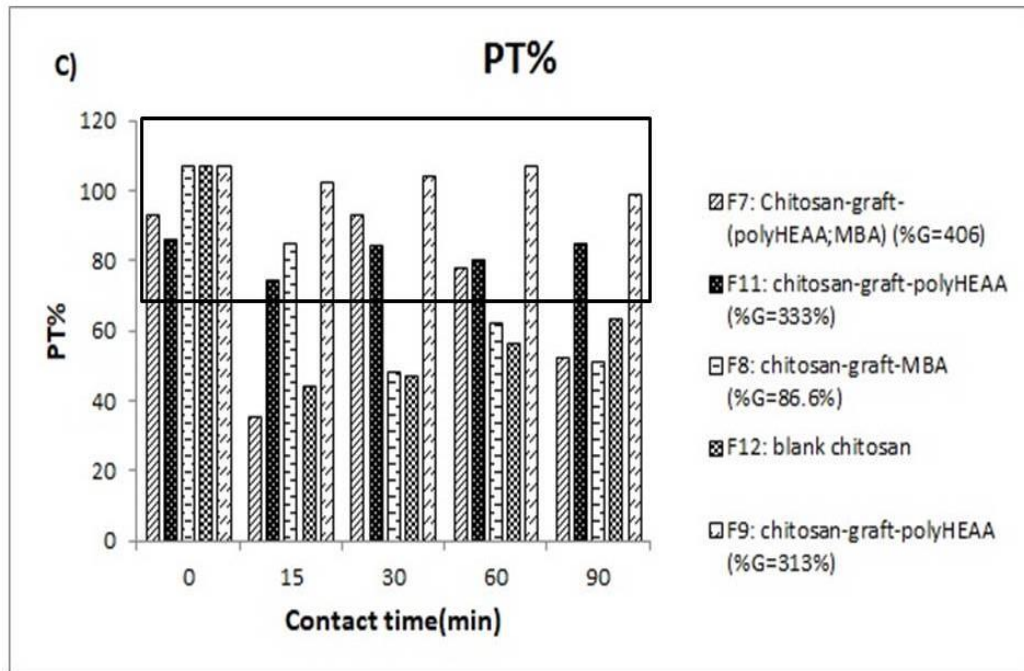
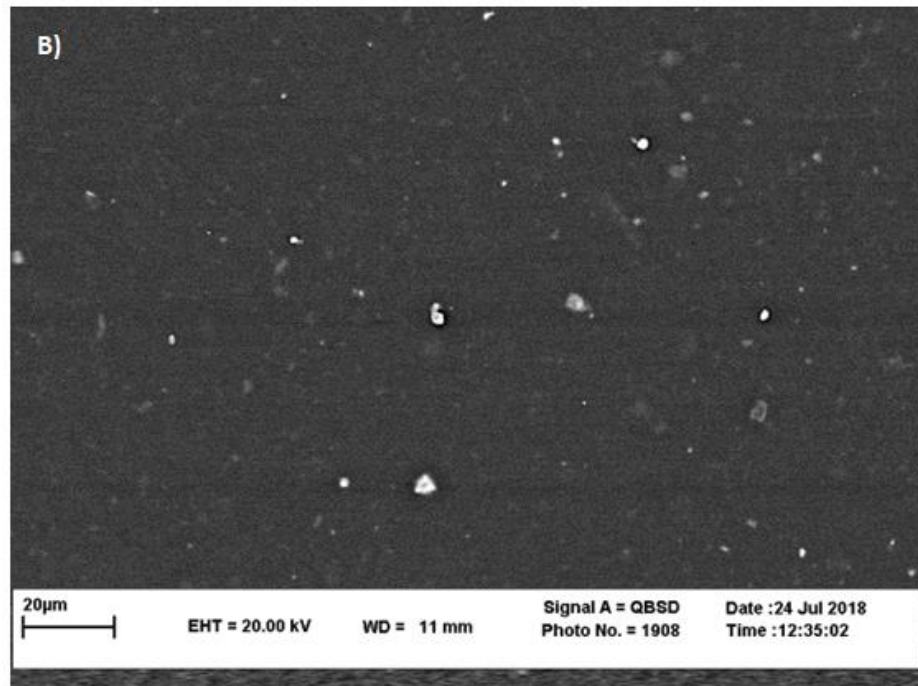
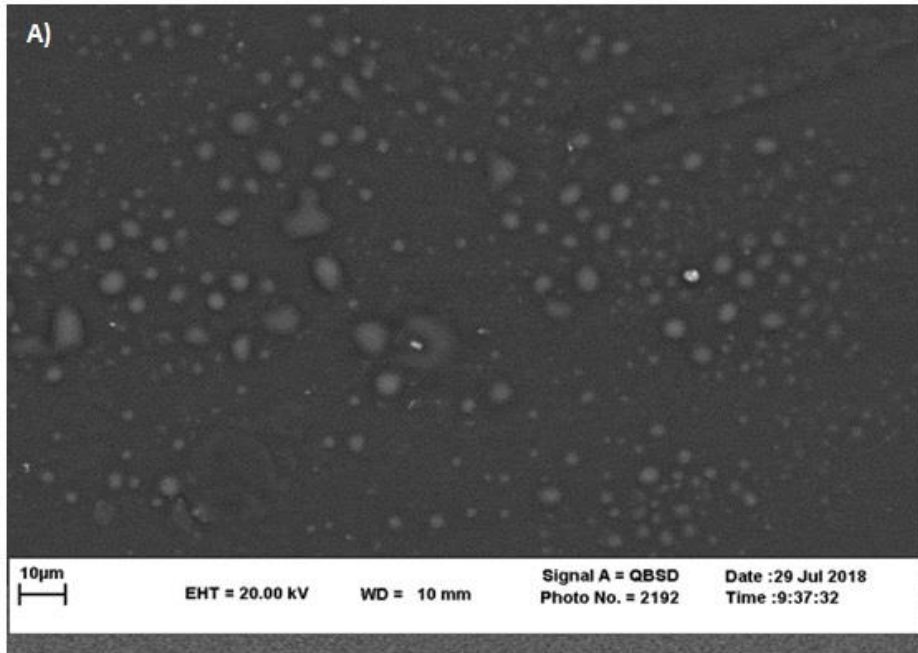


Figure 11: A) prothrombin time, B) international normalized ratio, C) PT percent, D) activated partial thromboplastin time for F7: chitosan-graft-(polyHEAA;MBA) (%G=406), F8: chitosan-graft-MBA (%G=86.6%), F9: chitosan-graft-polyHEAA (%G=313%) F11: chitosan-graft-polyHEAA (%G=333%), F12: blank chitosan

3.1.6 *In vitro* Blood Contact Test

The *in vitro* blood contact test was applied to obtain evidence on the blood-biomaterial contact properties of films. The surface morphologies of the samples after blood contact were examined using SEM micrographs with a magnification of 2000. The SEM images of the chitosan-*graft*-(polyHEAA;MBA) film (F7) given in Figure 12 (A) reveals water droplets entrapped within the polymer film showing the water absorbing and water locking characteristics of the polymer film. The surface of the same film after contact with platelet rich plasma or whole blood, Figure 12 (B) is not altered significantly apart from a decrease in size of the water droplets within the polymer film. Any significant evidence of platelet adhesion, or cell adhesion on the polymer surface could not be identified within the limitations of the experimental procedures applied. Chitosan film (F12) is shown in Figure 12 (C and D), before and after contact with platelet rich plasma. A comparison of the film surfaces before and after blood contact shows that the chitosan film surface is coated with a layer of plasma material. More hydrophilic surface of the grafted product may have hindered interaction with blood components.



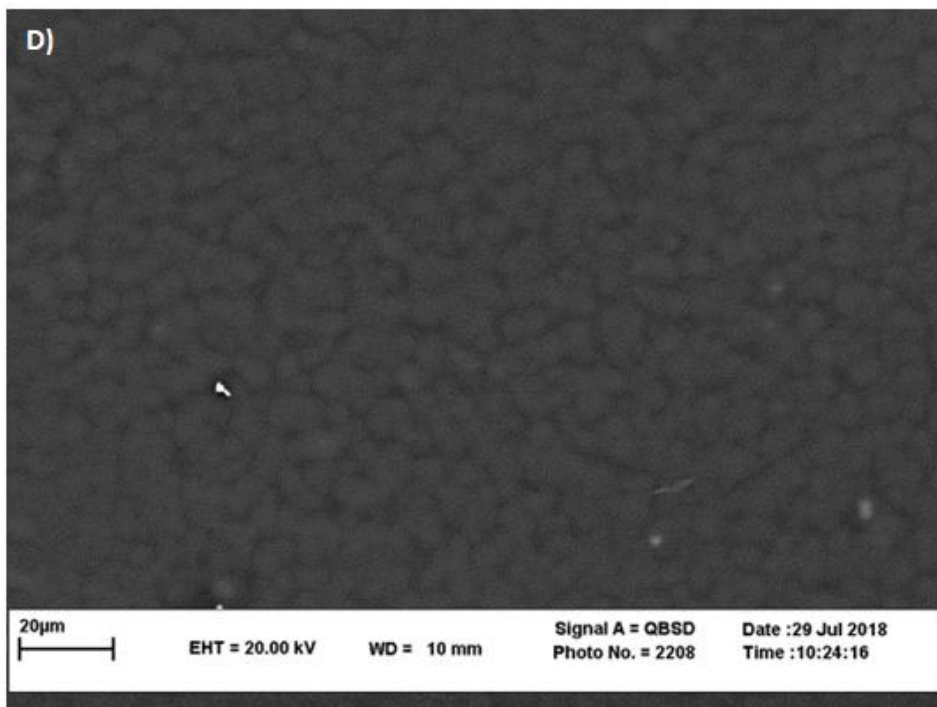
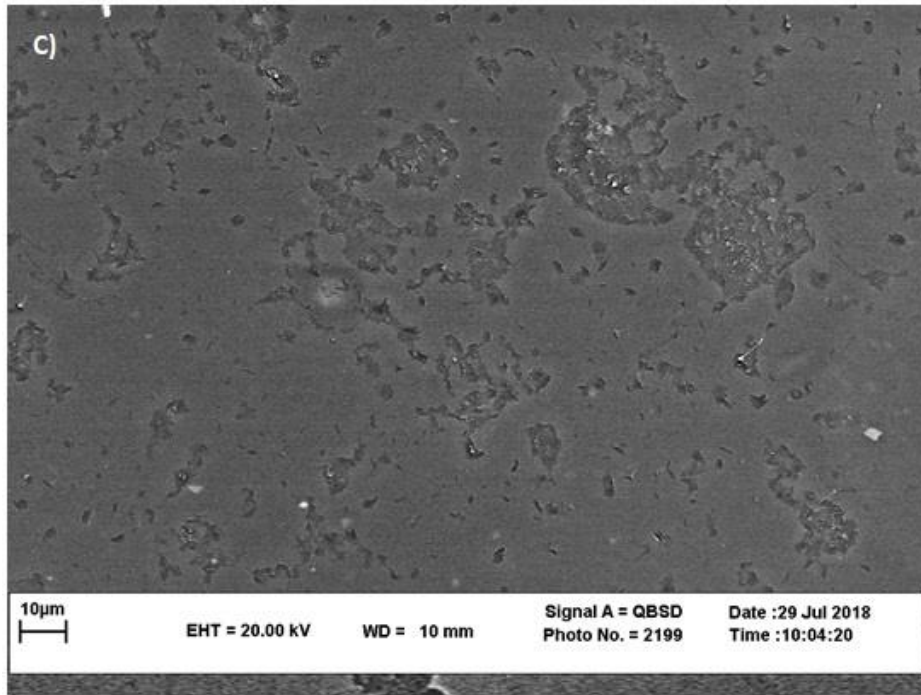


Figure 12: SEM images of A) chitosan-*graft*-(polyHEAA;MBA) film, B) chitosan-*graft*-(polyHEAA;MBA) film after contact with blood, C) chitosan, D) chitosan film after contact with blood.

3.1.7 Human Serum Albumin (HSA) Adsorption

The absorbance values of HSA solutions before and after contact with the chitosan-*graft*-polyHEAA films are given in Table 8. It can followed from the table that at all concentrations absorbance values decrease up to 3 h contact with the adsorbent revealing HSA adsorption onto the polymer films. After 3 h absorbances increase indicating desorption of the protein from the surface of the polymer. Therefore, data at 3h contac were taken to calculate the amount of adsorbed HSA onto the polymer as mg/g polymer. In Table 9 the equilibrium adsorption values for HSA are shown. The adsorbed amounts of HSA reported in Table 10 correspond to %removal from solution.

Table 8: Spectrophotometric Data for HSA adsorption

F9				
Time (h)	Absorbance			
1	0.246	0.222	0.224	0.215
2	0.284	0.25	0.245	0.211
3	0.24	0.229	0.228	0.205
4	0.268	0.248	0.197	0.218
5		0.236	0.218	0.209

F8				
Time (h)	Absorbance			
1	0.219	0.244	0.227	0.214
2	0.251	0.229	0.21	0.216
3	0.23	0.231	0.238	0.21
4	0.261	0.235	0.249	0.228
5	0.265	0.251	0.239	0.224

F7				
Time (h)	Absorbance			
1	0.252	0.231	0.221	
2	0.245	0.248	0.222	0.2
3	0.228	0.222	0.216	
4	0.263	0.251	0.232	0.209
5	0.263	0.253	0.227	0.211

F11				
Time (h)	Absorbance			
1	0.26	0.232	0.208	0.218
2	0.255	0.231	0.21	0.215
3	0.23	0.285	0.217	0.211
4	0.273	0.231	0.221	0.215
5	0.262	0.247	0.231	0.216

F12				
Time (h)	Absorbance			
1	0.261	0.232	0.209	0.214
2	0.258	0.223	0.209	0.21
3	0.227	0.228	0.211	0.211
4	0.254	0.225	0.21	0.226
5	0.258	0.235	0.217	0.219

Table 9: HSA Adsorption capacities of the chitosan-*graft*-polyHEAA samples at 3h contact in different initial concentrations

Concentration mg/mL	F12	F11	F7	F8
3.00	49	45	49	45
1.50	9.7	9.7	9.0	9.0
0.750	8.1	5.5	5.5	8.0
0.375	5.5	5.5	5.5	5.5

3.2 Chitosan-*graft*-(PHEAA; GA) Films

At 50°C when amount of monomer and crosslinker increases more percent grafting is recorded.

Table 10: Synthesis of chitosan-*graft*-(PHEAA; GA) films at 50°C

Sample ID	HEAA monomer (mL)	GA (mL)	Wt product(g) 50°C	Grafting% 50°C
G1	0.3	0.1	0.49	226
G2	0.9	0.1	1.03	586
G3	B	0.1	0.21	40
G4	0.3	0.3	0.47	213
G5	0.9	0.3	1.10	633
G6	-	0.3	0.26	73.3
G7	0.3	-	0.41	173

G8	0.9	-	0.81	440
G9	-	-	0.15	0

3.2.1 FT-IR Analysis of Chitosan-graft-(PHEAA; GA)

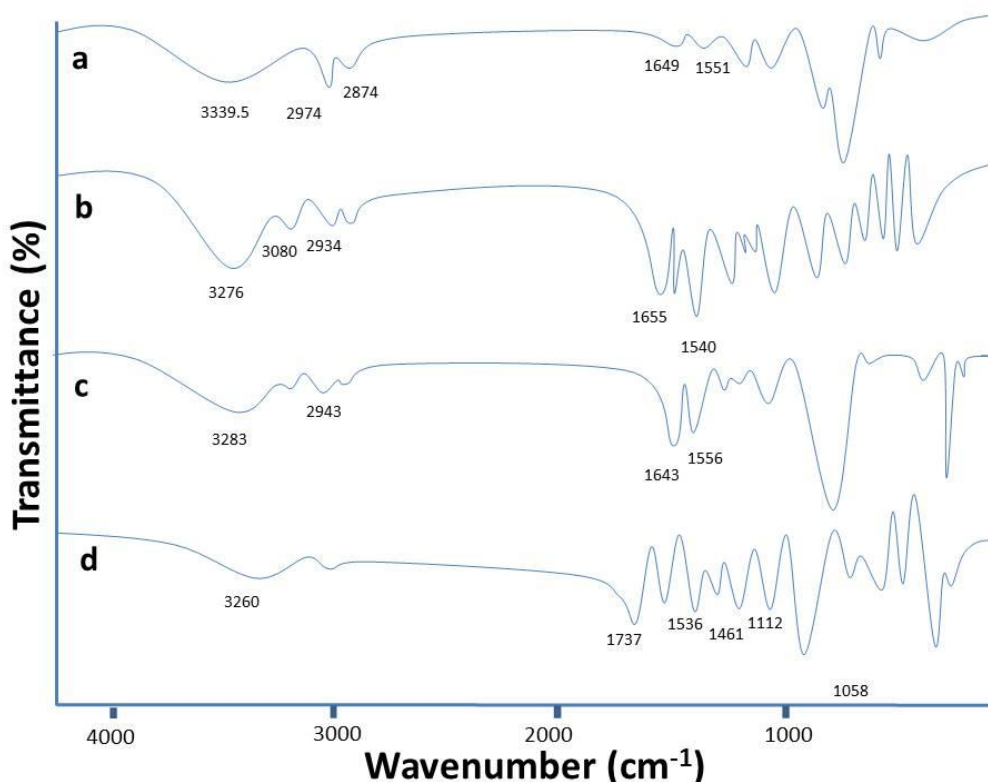


Figure 13: FTIR spectrum of (a) chitosan (b) PHEAA (c) chitosan-graft-PHEAA (d) chitosan-graft-(PHEAA; GA)

In the FTIR spectrum of chitosan shown in Figure 13(a), a characteristic Amide band at 1649 cm^{-1} , the C-H bending vibrations $1400\text{--}1500\text{ cm}^{-1}$ region, the -CH₃ bending at 1380 cm^{-1} , C-H stretching at 2884 and 2974 and H bonding at 3339.5 cm^{-1} are observable. The hydroxyethyl acrylamide (HEAA) spectrum in Figure 13(b) exhibits all characteristic absorption bands of -C-C-, -C=C-, C-H, C-O and O-H stretching. Chitosan-graft-PHEAA shown in Figure 13(c) exhibits the

absorption bands at 1643 cm^{-1} , which have been taken as evidence of amide bond formation between chitosan and HEAA. 3260 cm^{-1} in figure 13 (d) shows O-H stretching and 1737 cm^{-1} indicates carbonyl group for Chitosan-*graft*-(PHEAA; GA).

3.2.2 XRD Analysis of Chitosan-*graft*-(PHEAA; GA)

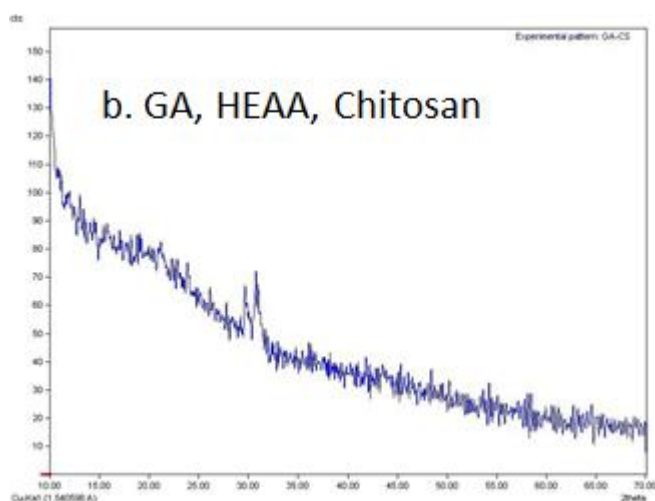


Figure 14: XRD analysis for b) chitosan-*graft*-(PHEAA; GA)

XRD pattern of film sample Chitosan-*graft*-(PHEAA; GA) is given in Figure 14. It has an amorphous nature.

3.2.3 SEM Analysis for Chitosan-*graft*-(PHEAA; GA)

The surface morphologies of grafted products were examined using SEM analysis given in Figure 15. All samples have smooth surfaces with some uncrosslinked chitosan adhering on the surfaces of the films.

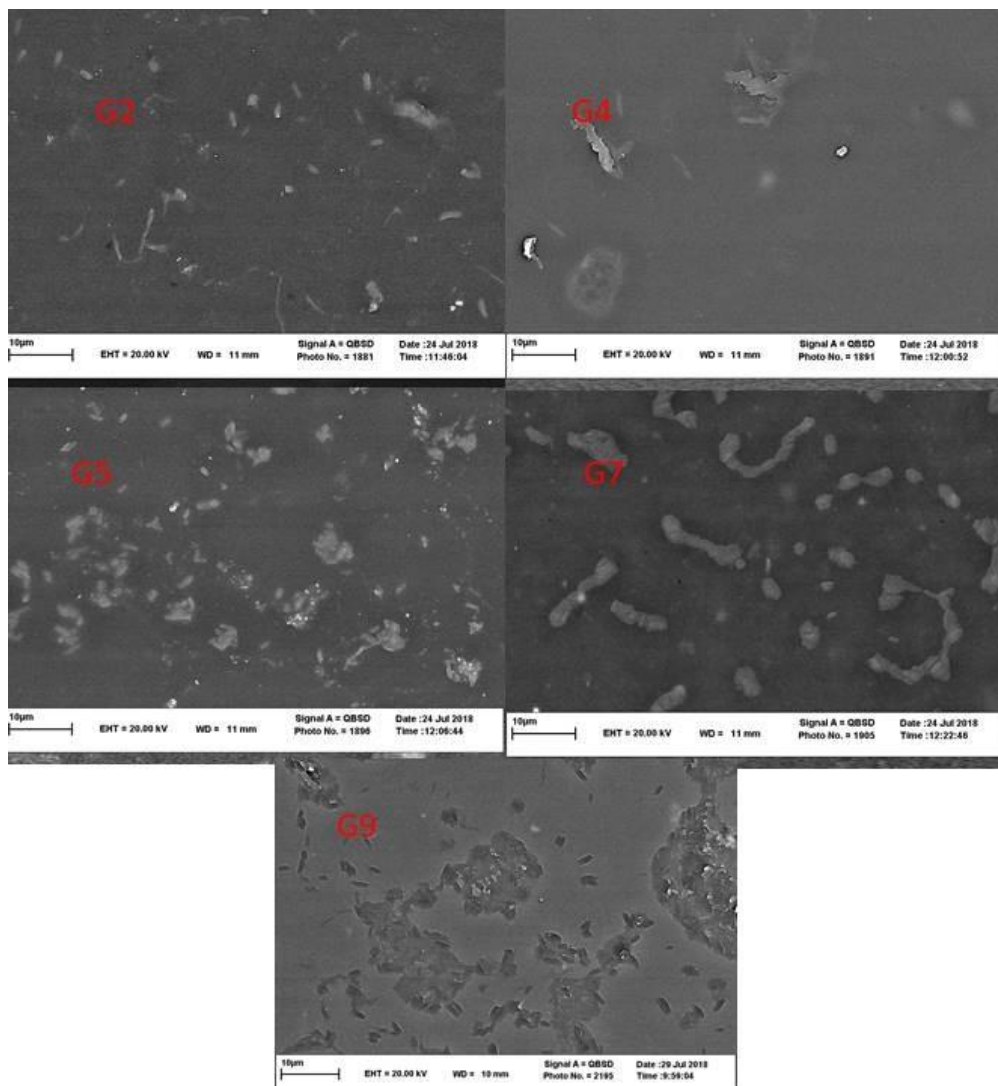


Figure 15: SEM images (5000X) of G2) chitosan-*graft*-(polyHEAA;GA) (%G=586%), G4) chitosan-*graft*-(polyHEAA;GA) (%G=213), G5) chitosan-*graft*-(polyHEAA;GA) (%G=633), G7) chitosan-*graft*-polyHEAA (%G=173%), G9) chitosan.

3.2.4 Elemental Analysis of Chitosan-graft-(PHEAA; GA)

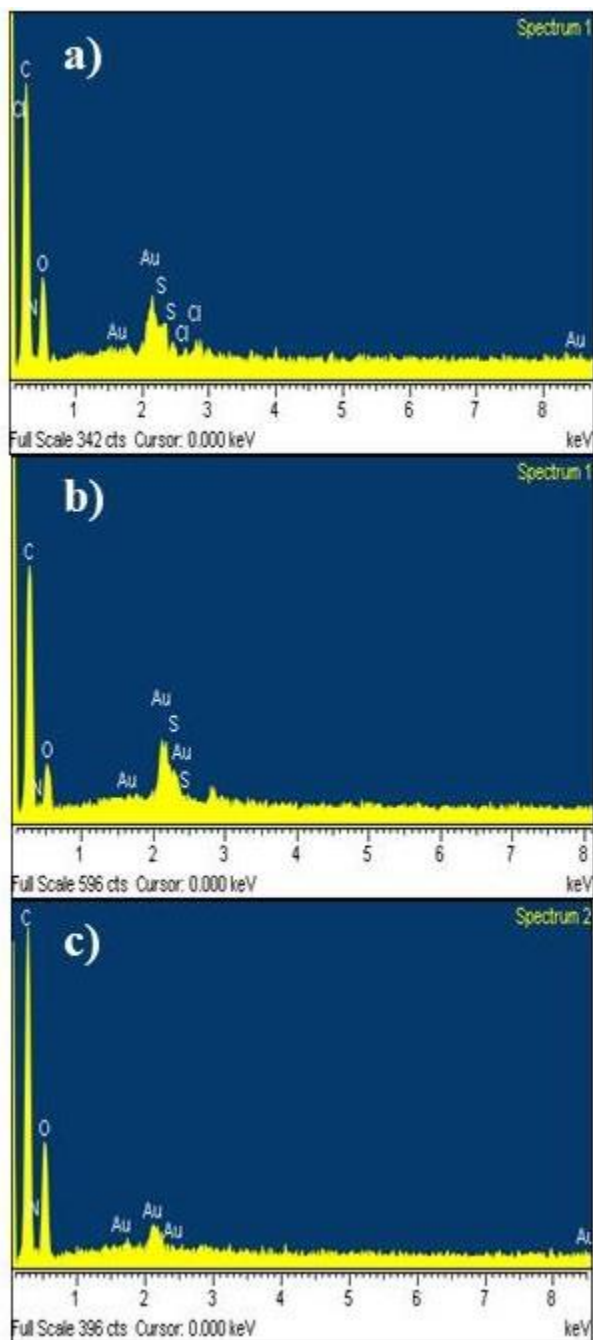


Figure 16: elemental analysis for a) G1: chitosan-graft-(PHEAA; GA), b) G4: chitosan-graft-(PHEAA; GA), c) G9: chitosan

Table 11: Elemental analysis (Weight %) of chitosan-*graft*-(PHEAA; GA) samples (G1, G4, G9)

Sample ID	C%	N%	O%	S%	Cl%
G1	51.48	13.08	33.25	1.7	0.49
G4	56.2	13.79	27.99	2.01	0
G9	47.1	12.16	40.74		

Elemental analysis of the GA crosslinked and polyHEAA grafted samples G1 and G4 compared to that of chitosan only G9, shows that grafting of polyHEAA onto chitosan and crosslinking by GA are reflected by an increase in N% value together with an increase in C% accompanied by a decrease in O%.

3.2.5 Swelling Behaviour of Chitosan-*graft*-polyHEAA and Chitosan-*graft*-(polyHEAA;GA) Films

Swelling behaviour of chitosan-*graft*-(polyHEAA;GA) films (G1-G9) are illustrated in table 11 a-i and figure 17 a-i with 15% error. All samples reach a maximum swelling degree, which reduces to the equilibrium % swelling value within one and half hour contact with aqueous solution. Thermally cross-linked chitosan-*graft*-polyHEAA samples (G7, G8) with %G=173 and %G=440 exhibit equilibrium swelling degrees much higher than their GA crosslinked counterparts, namely G2, G3 and G5, G6. G7 swells to 460% and G8 to 282% within two hours of contact with pH=7.4 buffer solution. Thermally crosslinked chitosan (G9) alone has an equilibrium swelling capacity of 150%. Therefore, the effect of grafted polyHEAA on increasing hydrophilicity and water retention capacity of chitosan is clearly observable. The film formed by the chitosan; sample G9, disintegrated due to the presence of amine functionality on the chain backbone. The results reveal that cross-

linking chitosan via grafting by a difunctional crosslinker, GA, causes a decrease in the swelling ability at pH 7.4.

Table 12: Swelling behavior over time for G1: chitosan-*graft*-(polyHEAA;GA) (%G=226), G2: chitosan-*graft*-(polyHEAA;GA) (%G=586%), G3: chitosan-crosslinked-GA (%G=40), G4: chitosan-*graft*-(polyHEAA;GA) (%G=213), G5: chitosan-*graft*-(polyHEAA;GA) (%G=633), G6: chitosan-crosslinked-GA (%G=73.3), G7: chitosan-*graft*-polyHEAA (%G=173%), G8: chitosan-*graft*-polyHEAA (%G=440), G9: chitosan at pH 7.4

	time	%Swelling
G1	0	0
	30	126
	60	129
	90	83
	120	61
	time	%Swelling
G2	0	0
	30	178
	60	181
	90	175
	120	190

	time	%Swelling
G3	0	0
	30	49
	60	50
	90	15
	120	70

	time	%Swelling
G4	0	0
	30	101
	60	62
	90	46
	120	60

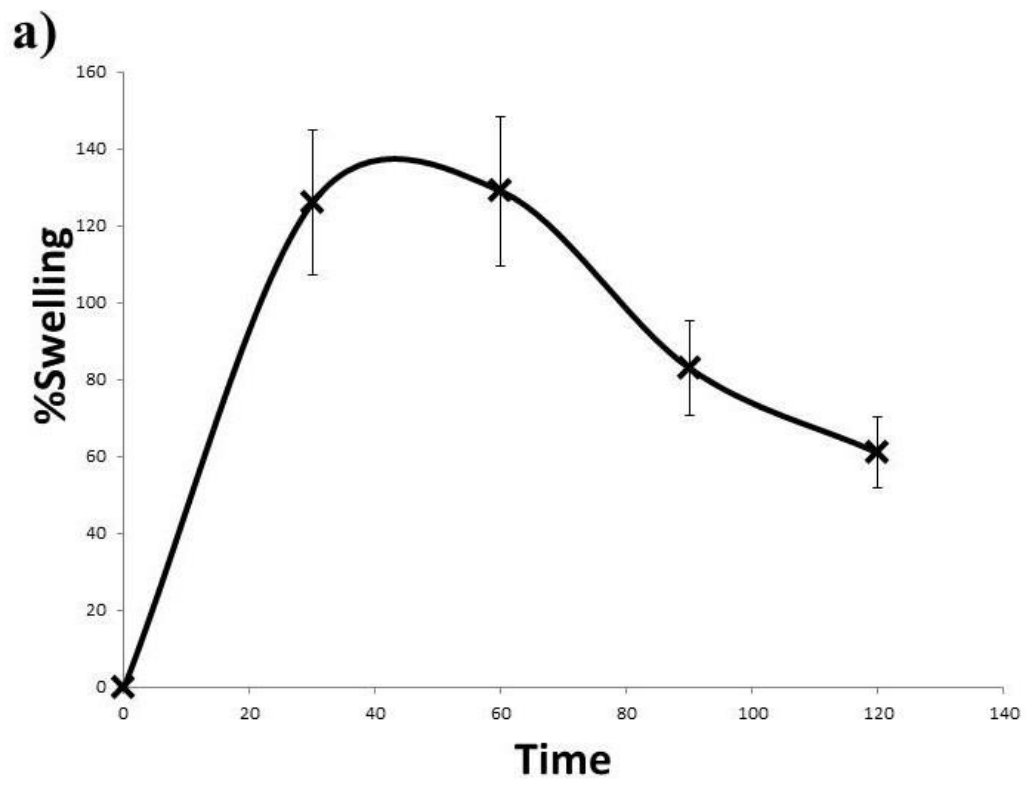
	Time	%Swelling
G5	0	0
	30	136
	60	86
	90	97
	120	93

	Time	%Swelling
G6	0	0
	30	73
	60	37
	90	52
	120	120

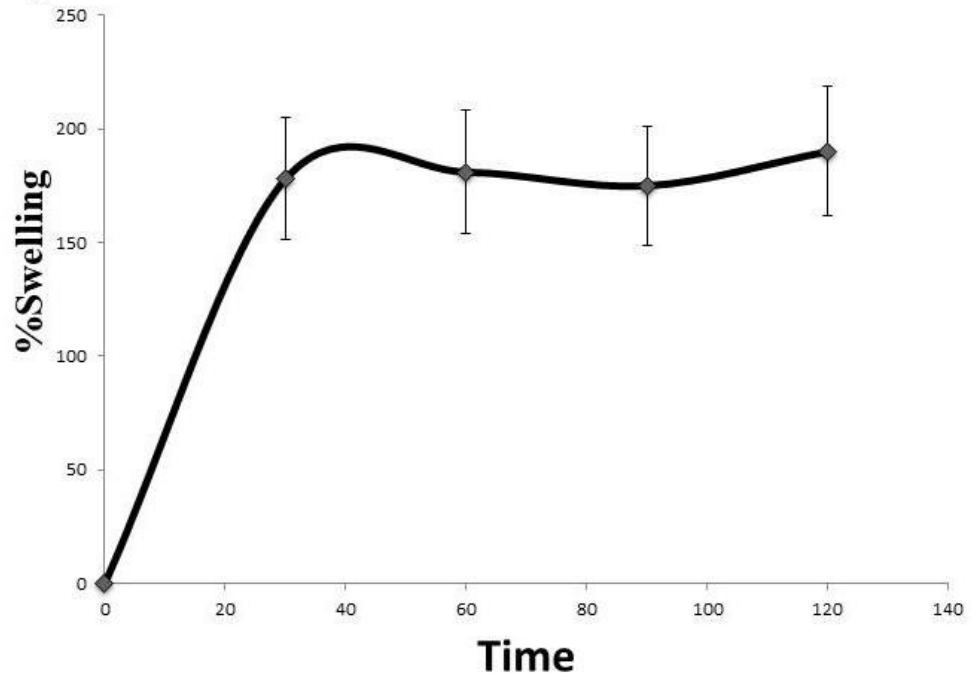
	Time	%Swelling
G7	0	0
	30	325
	60	611
	90	460
	120	463

	Time	%Swelling
G8	0	0
	30	312
	60	380
	90	282
	120	298

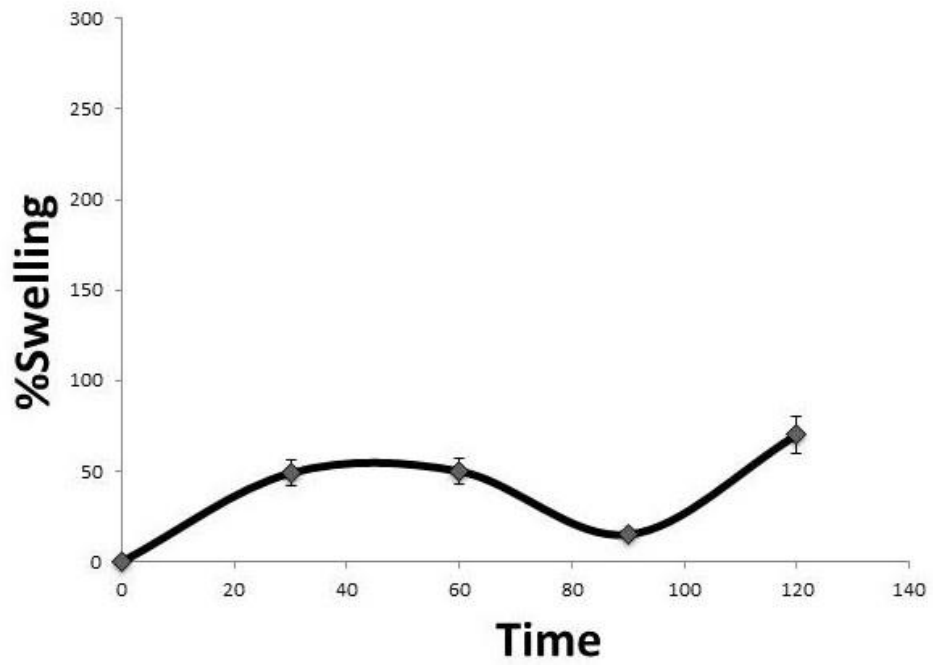
	Time	%Swelling
		0
G9	30	185
	60	219
	90	135
	120	135

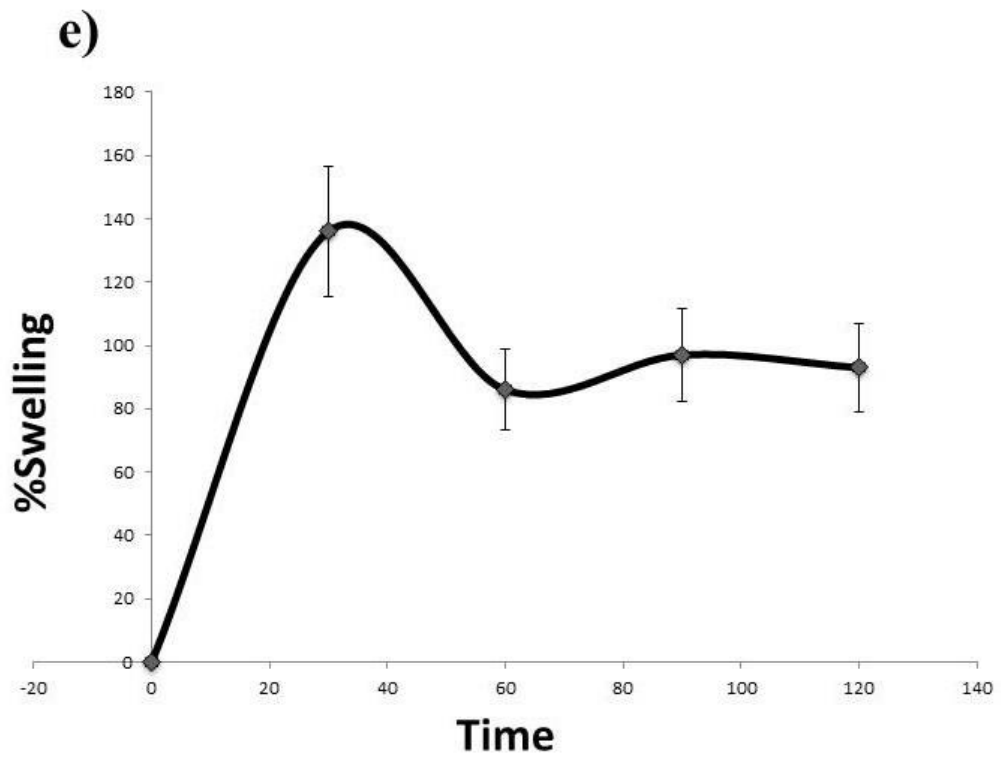
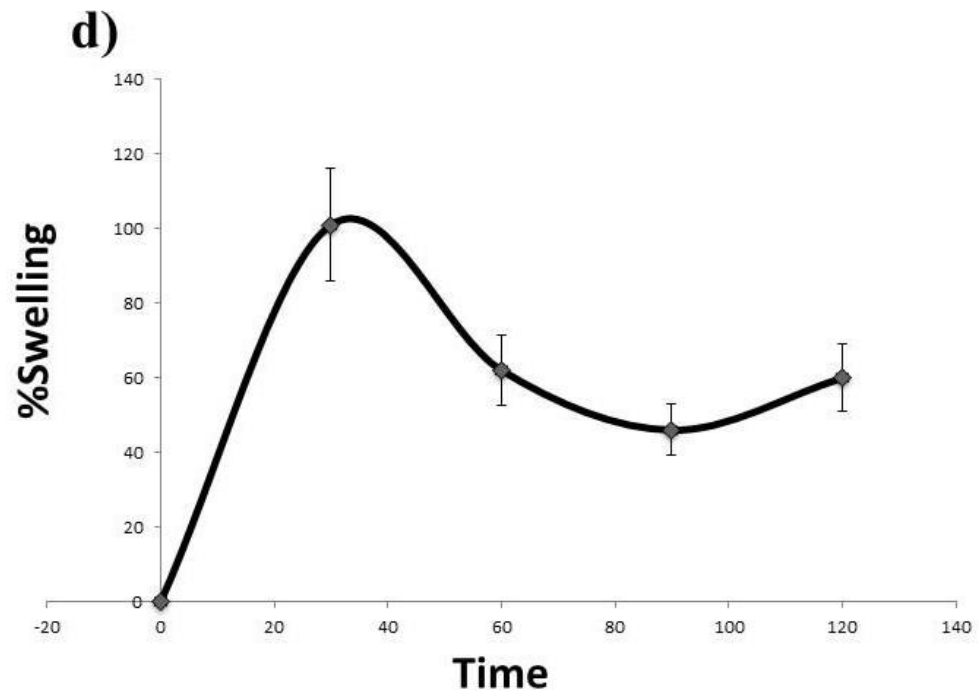


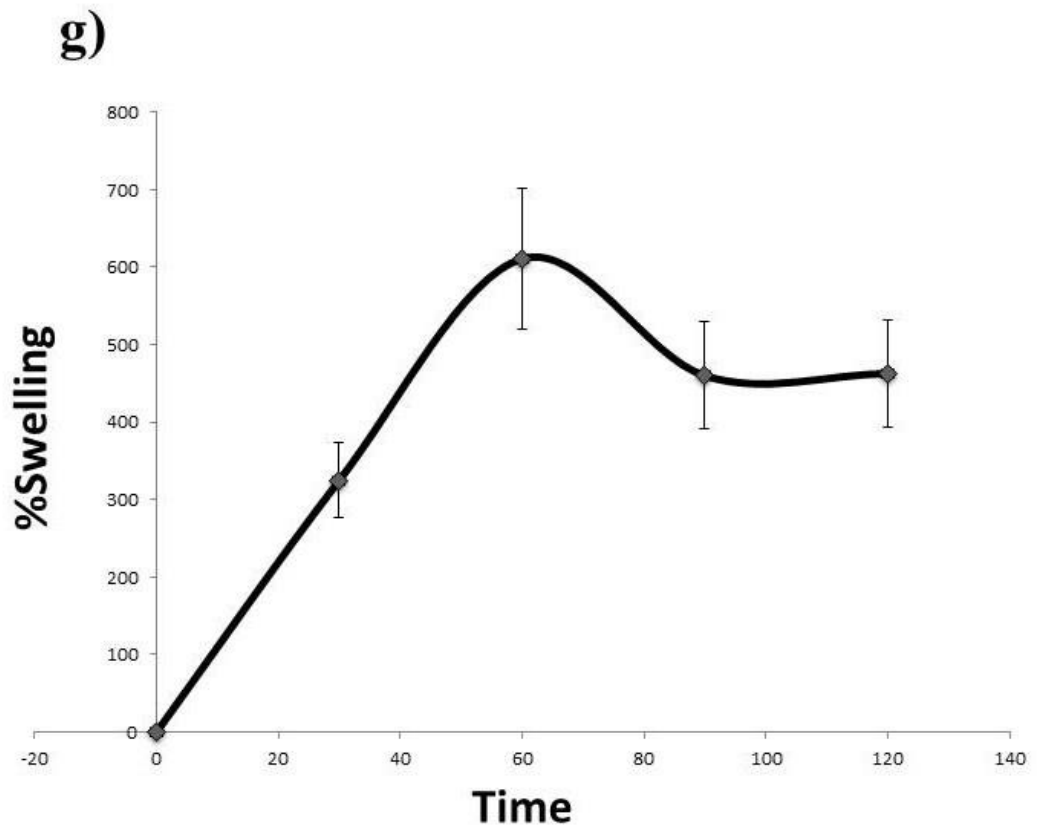
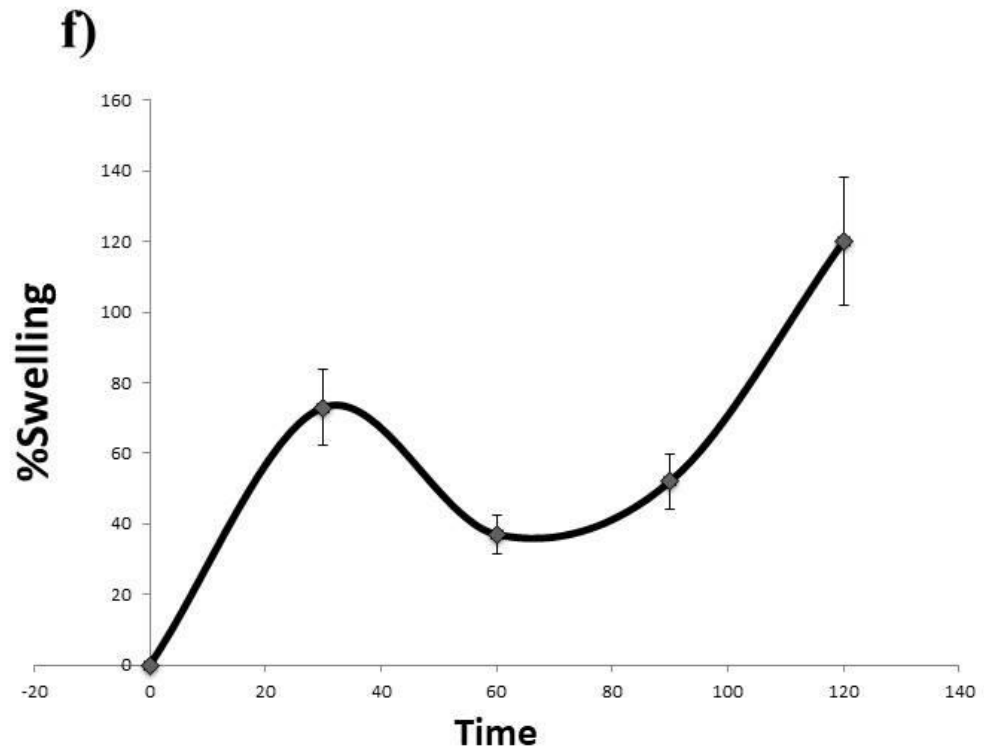
b)

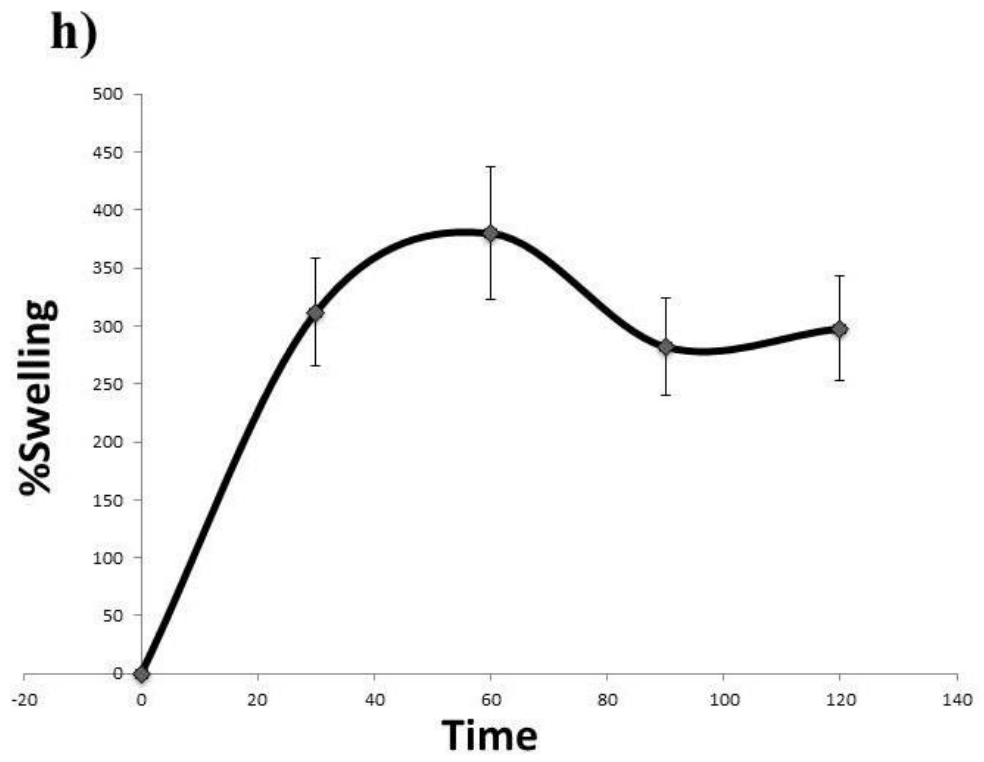


c)









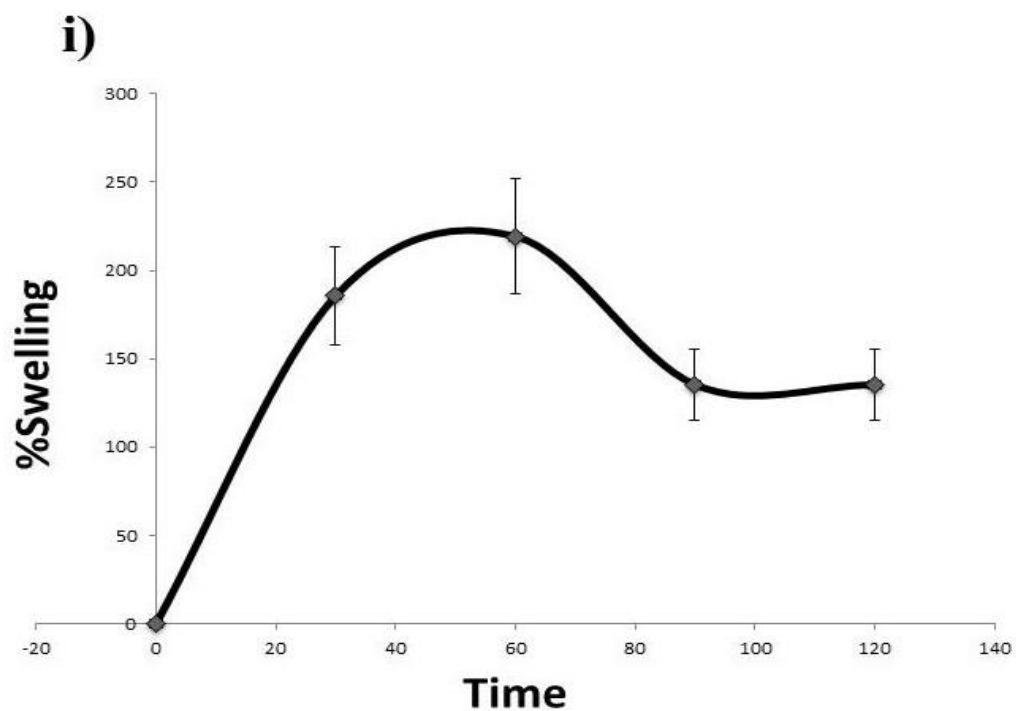


Figure 17: Swelling behavior over the time for a) G1: chitosan-*graft*-(polyHEAA;GA) (%G=226), b) G2: chitosan-*graft*-(polyHEAA;GA) (%G=586%), c) G3: chitosan-crosslinked-GA (%G=40), d) G4: chitosan-*graft*-(polyHEAA;GA) (%G=213), e) G5: chitosan-*graft*-(polyHEAA;GA) (%G=633), f) G6: chitosan-crosslinked-GA (%G=73.3), g) G7: chitosan-*graft*-polyHEAA (%G=173%), h) G8: chitosan-*graft*-polyHEAA (%G=440), i) G9: chitosan at pH 7.4

3.2.6 Iron (Fe³⁺) Adsorption

The calibration for FeCl₃ solutions obtained by uv-vis spectrophotometry is given in Figure 18. Fe³⁺ adsorption data of the GA crosslinked chitosan-*graft*-polyHEAA films are given in Table 12 and Figure 19. In dilute solutions of Fe³⁺ (125 and 250 ppm) adsorption that occurs during the first hour of contact is followed by desorption during the second hour. Finally after 24 h, when sufficiently long time was allowed for adsorbent- Fe³⁺ contact, the adsorption capacity increased to a level comparable to that at 1h contact. In more concentrated Fe³⁺ solutions (375 and 500 ppm) for the first 2 hours, adsorption capacity increased but then either increased slightly or stayed constant and equilibrated after 24 h. Sample G7 and G8 have an equilibrium adsorption capacity of 27.9 mg/g and 39.4 mg/g respectively in 500 ppm solution. The corresponding values for the GA crosslinked counterparts G1 and G2 are 35.6 mg/g and 44.8 mg/g and those for G2 and G5 are 44.8 mg/g and G5 30.6 mg/g respectively. As can be followed from the data provided, in general, less crosslinking and higher swelling capacity together with higher grafting value of polyHEAA lead to higher adsorption capacity. The optimum sample is G2 with 44.8 mg/g adsorption capacity at 500 ppm at pH=1.2.

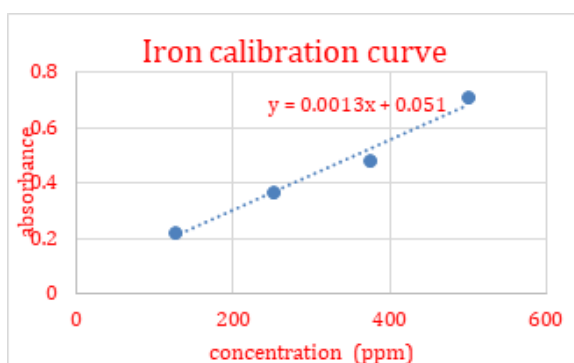


Figure 18: calibration curve for Iron solutions

Table 13: Adsorbed mass (mg) of Fe³⁺ for G1: chitosan-*graft*-(polyHEAA;GA) (%G=226), G2: chitosan-*graft*-(polyHEAA;GA) (%G=586%), G3: chitosan-crosslinked-GA (%G=40), G4: chitosan-*graft*-(polyHEAA;GA) (%G=213), G5: chitosan-*graft*-(polyHEAA;GA) (%G=633), G6: chitosan-crosslinked-GA (%G=73.3), G7: chitosan-*graft*-polyHEAA (%G=173%), G8: chitosan-*graft*-polyHEAA (%G=440), G9: blank chitosan

G1

Time (h)	500ppm	375ppm	250ppm	125ppm
1	23.0	17.0	12.6	2.1
2	27.7	23.6	2.6	2.5
24	35.5	24.5	18.4	5.9

G2

Time (h)	500ppm	375ppm	250ppm	125ppm
1	21.7	15.8	14.9	0
2	22.7	22.1	7.2	4.8
24	44.8	20.0	19.5	4.3

G3

Time (h)	500ppm	375ppm	250ppm	125ppm
1	20.2	13.5	10.4	5.5
2	26.4	23.5	10.9	0
24	34.0	19.2	15.3	3.0

G4

Time (h)	500ppm	375ppm	250ppm	125ppm
1	21.5	12.9	9.4	6.5
2	24.8	24.9	5.0	1.9
24	28.8	19.2	17.0	2.1

G5

Time (h)	500ppm	375ppm	250ppm	125ppm
1	19.2	16.4	8.4	4.0
2	21.9	20.2	3.6	0
24	30.6	19.6	13.9	5.2

G6

Time (h)	500ppm	375ppm	250ppm	125ppm
1	20.5	8.1	7.9	4.0
2	24.6	21.9	6.0	3.4
24	16.8	9.7	14.8	6.5

G7

Time (h)	500ppm	375ppm	250ppm	125ppm
1	25.5	10.2	13.2	5.0
2	21.9	21.0	7.2	0
24	27.9	30.2	21.6	8.1

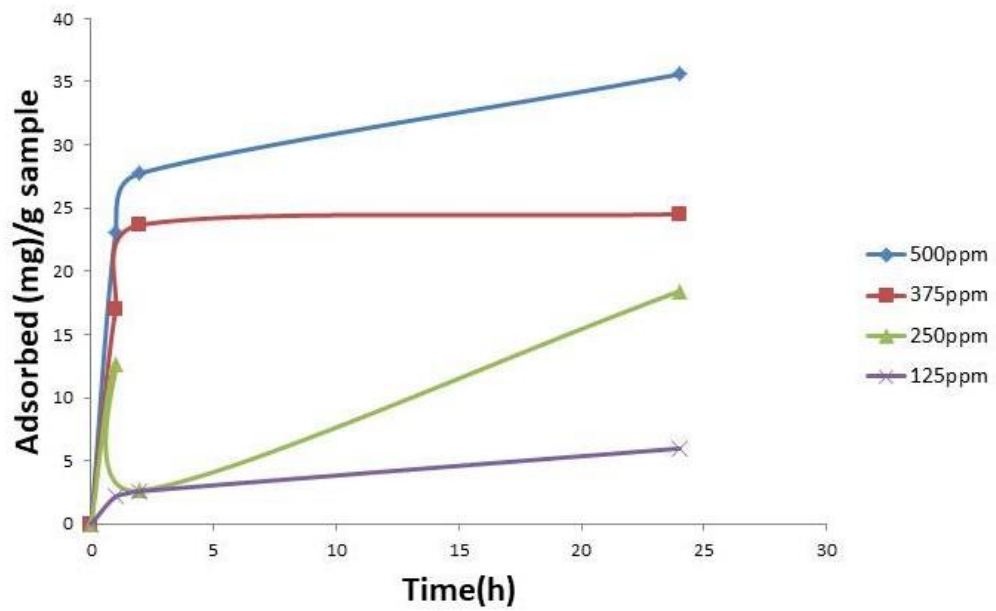
G8

Time (h)	500ppm	375ppm	250ppm	125ppm
1	20.0	14.5	12.7	6.1
2	31.9	26.9	12.0	2.9
24	39.4	29.5	21.7	7.6

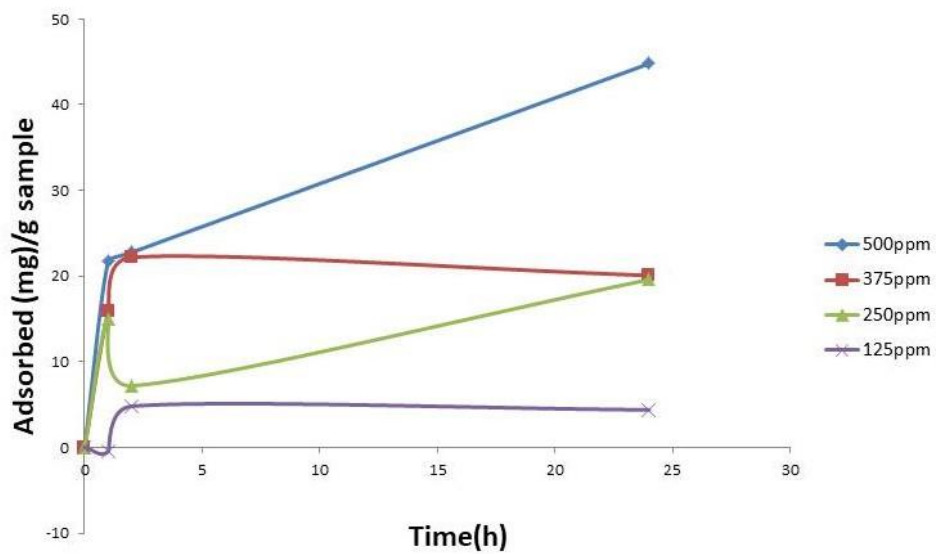
G9

Time (h)	500ppm	375ppm	250ppm	125ppm
1	11.9	14.9	9.0	7.0
2	26.4	25.1	6.4	2.3
24	36.9	26.7	16.3	7.4

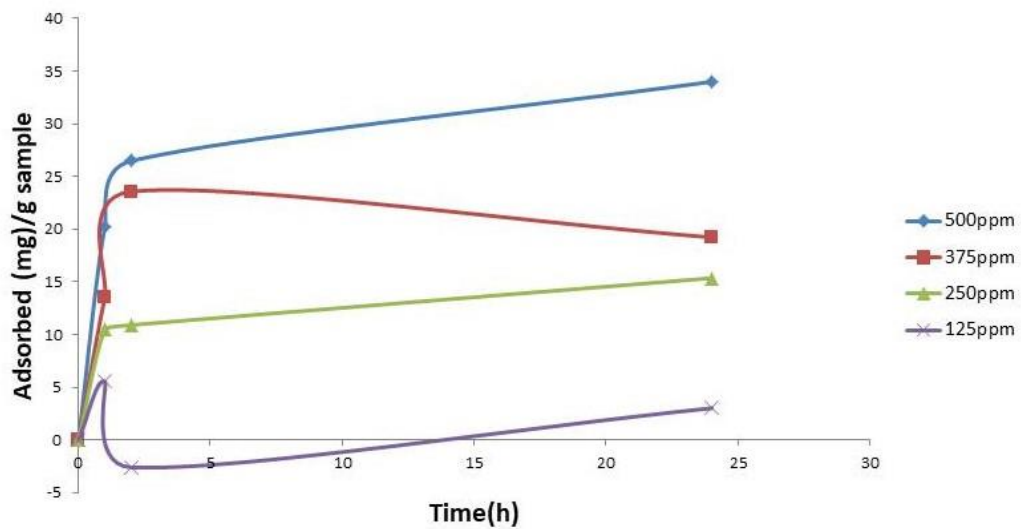
G1



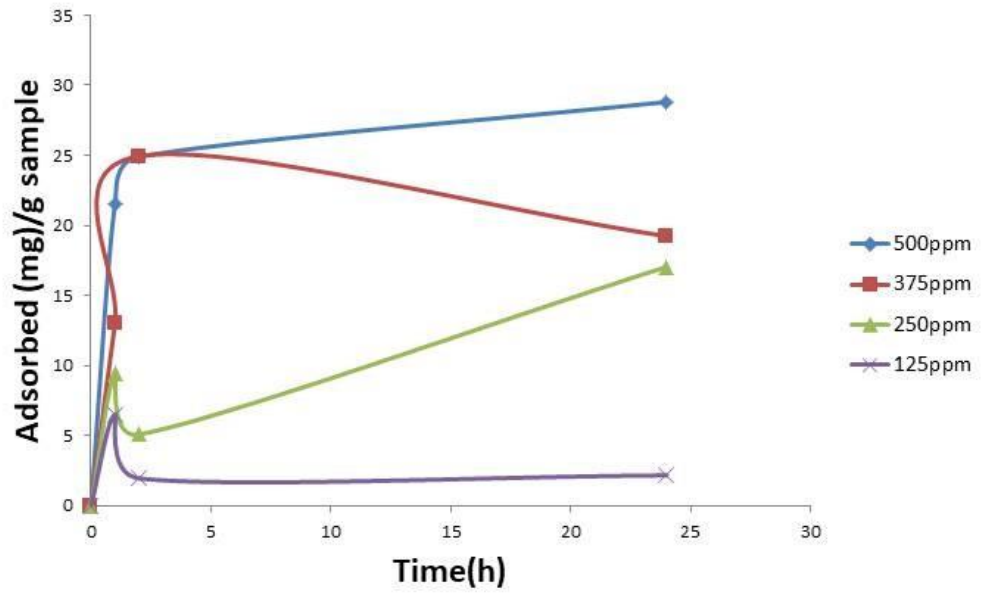
G2



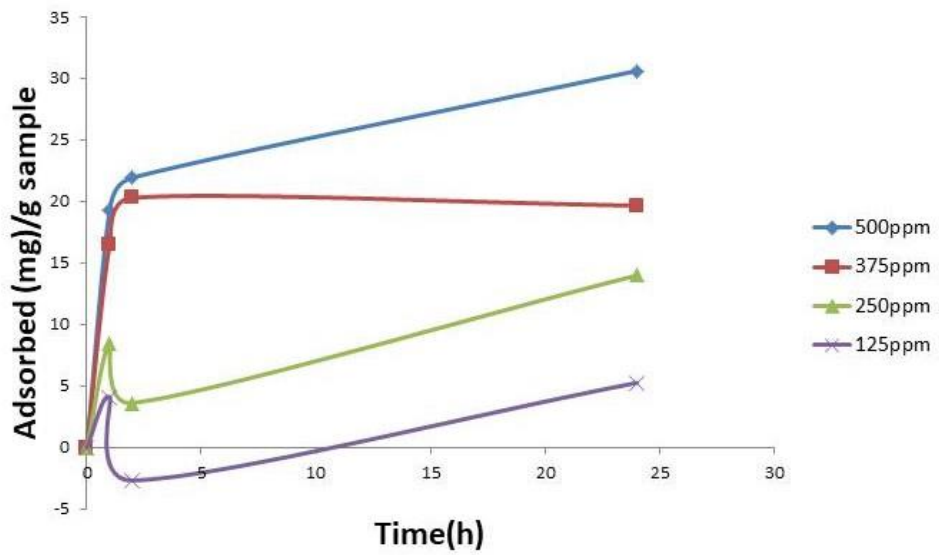
G3



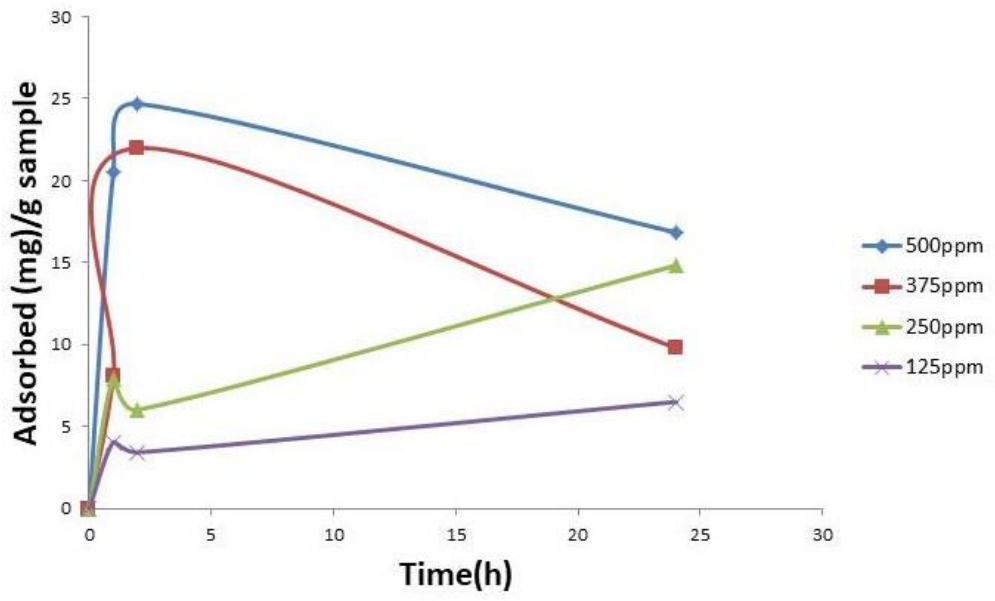
G4



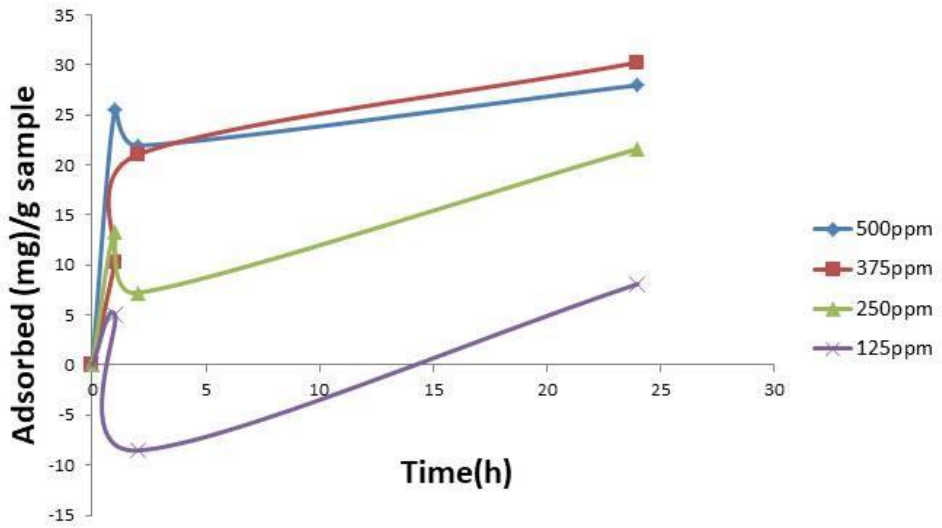
G5



G6



G7



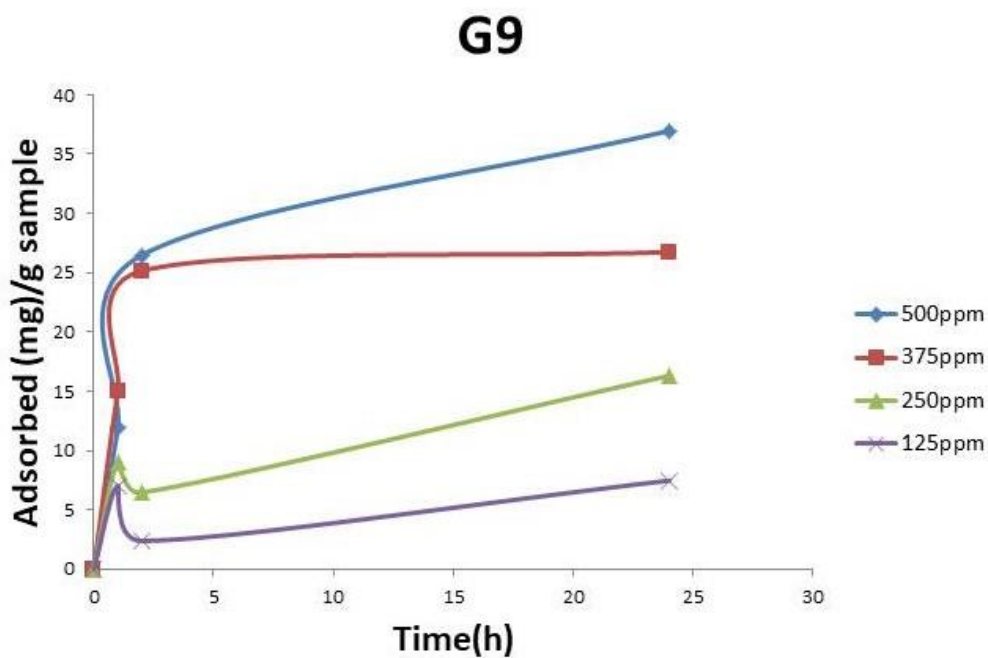
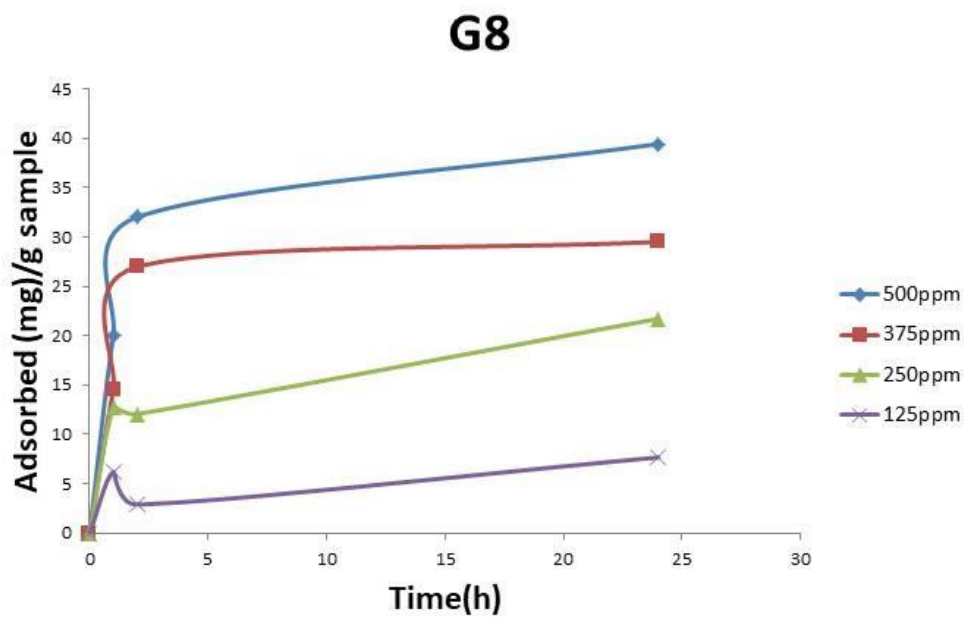


Figure 19: Adsorbed mass (mg) of Fe^{3+} for G1: chitosan-*graft*-(polyHEAA;GA) (%G=226), G2: chitosan-*graft*-(polyHEAA;GA) (%G=586%), G3: chitosan-crosslinked-GA (%G=40), G4: chitosan-*graft*-(polyHEAA;GA) (%G=213), G5: chitosan-*graft*-(polyHEAA;GA) (%G=633), G6: chitosan-crosslinked-GA (%G=73.3), G7: chitosan-*graft*-polyHEAA (%G=173%), G8: chitosan-*graft*-polyHEAA (%G=440), G9: chitosan

Table 14: Grafting percentages, swelling percentages and Iron adsorption capacities for G1: chitosan-graft-(polyHEAA;GA) (%G=226), G2: chitosan-graft-(polyHEAA;GA) (%G=586%), G3: chitosan-crosslinked-GA (%G=40), G4: chitosan-graft-(polyHEAA;GA) (%G=213), G5: chitosan-graft-(polyHEAA;GA) (%G=633), G6: Chitosan-crosslinked-GA (%G=73.3), G7: chitosan-graft-polyHEAA (%G=173%), G8: chitosan-graft-polyHEAA (%G=440), G9:chitosan

	G1	G2	G3	G4	G5	G6	G7	G8	G9
GA (mL)	0.1	0.1	0.1	0.3	0.3	0.3	B	B	B
G%	226	586	40	213	633	73.3	173	440	0
Swelling%	83	175	15	46	97	52	460	282	135
Adsorption Capacity	35.6	44.8	34	28.8	30.6	16.8	27.9	39.4	36.9

3.2.6.1 SEM Analysis for Fe³⁺ Adsorption

Figure 20 (a) and (b) shows SEM images for chitosan-graft-polyHEAA sample and the same sample after contact with Fe³⁺ solution. The picture in Figure 20 (b) clearly shows iron adsorption on the surface of the film.

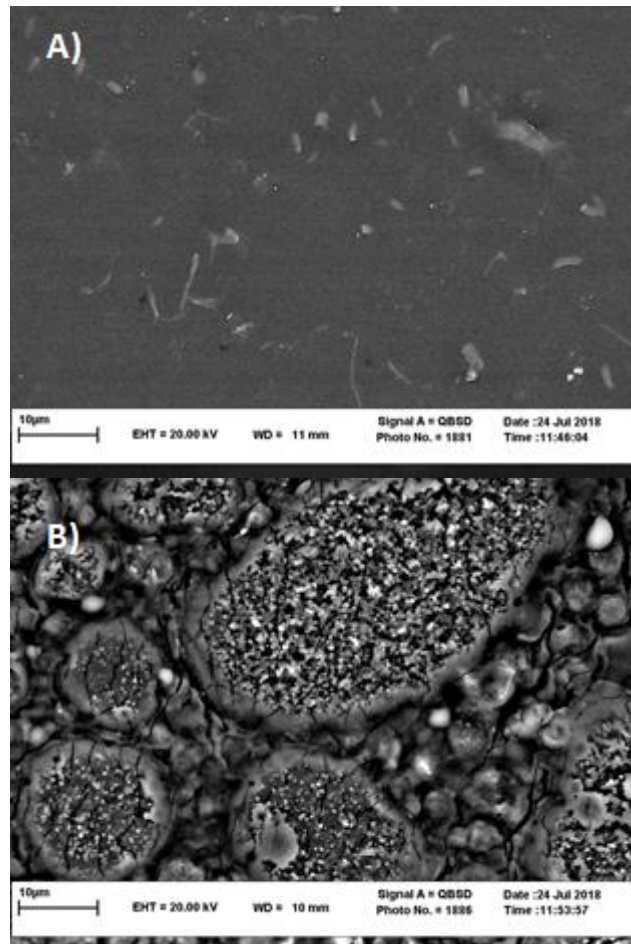


Figure 20: SEM images (5000X) of (a) chitosan-*graft*-(PHEAA; GA), (b) Fe³⁺ adsorbed chitosan-*graft*-(PHEAA; GA)

Chapter 4

CONCLUSION

Chitosan-*graft*-(polyHEAA;MBA) copolymers synthesized by free radical initiation in aqueous solution are hydrophilic polymers, which swell in aqueous media, and have limited protein adhesion property. They cause increased blood coagulation times upon contact with blood for up to 90 min, and provide less thrombogenic surface compared to chitosan. Thermally cross-linked chitosan-*graft*-polyHEAA films, on the other hand, do not produce any significant anticoagulant activity compared to chitosan alone or to MBA cross-linked films.

The synthesized Chitosan-*graft*-(PHEAA; GA) products adsorb Fe^{+3} over the time. Less crosslinking and higher swelling capacity causes higher adsorption. The amount of polyHEAA grafted also affects the Fe^{+3} adsorption capacity. The optimum sample is the one with light GA crosslinking with 586% grafting value and 180% equilibrium swelling capacity. The equilibrium Fe^{3+} adsorption capacity of the sample is 44.8 mg/g. Chitosan-*graft*-polyHEAA samples are promising Fe^{3+} chelators for the treatment of Fe^{3+} overload according to *in vitro* chemical analyses.

These preliminary results lead to the conclusion that chitosan-*graft*-polyHEAA films are potential candidates as hemocompatible materials and could be an alternative for chelating and anticoagulant agents. However, more detailed analyses are needed in this regard which deserve further testing.

Chapter 5

FUTURE DIRECTIONS

Blood contact properties of chitosan-*graft*-polyHEAA films were investigated in terms blood coagulation and iron adsorption tests. These materials should be further evaluated for full blood compatibility characterization and removal of excess iron from blood by further in-vitro and in-vivo tests. These materials have promising applications like chelating agents to adsorb overloaded Fe^{3+} from blood in patients who are diagnosed with thalassemia in addition to anticoagulant activity.

REFERENCES

- [1] Bandyopadhyay, A., & Bose, S. (Eds.). (2013). *Characterization of Biomaterials*. Newnes.
- [2] Chen, L., Han, D., & Jiang, L. (2011). On improving blood compatibility: from bioinspired to synthetic design and fabrication of biointerfacial topography at micro/nano scales. *Colloids and Surfaces B: Biointerfaces*, 85(1), 2-7.
- [3] Labarre, D. (2001). Improving blood compatibility of polymeric surfaces. *Trends Biomater Artif Organs*, 15, 1-3.
- [4] Gorbet, M. B., & Sefton, M. V. (2004). Biomaterial-associated thrombosis: roles of coagulation factors, complement, platelets and leukocytes. *Biomaterials*, 25(26), 5681-5703.
- [5] Ostuni, E., Chapman, R. G., Holmlin, R. E., Takayama, S., & Whitesides, G. M. (2001). A survey of structure– property relationships of surfaces that resist the adsorption of protein. *Langmuir*, 17(18), 5605-5620.
- [6] Liu, Z., Jiao, Y., Wang, T., Zhang, Y., & Xue, W. (2012). Interactions between solubilized polymer molecules and blood components. *Journal of Controlled Release*, 160(1), 14-24.

- [7] Mao, C., Qiu, Y., Sang, H., Mei, H., Zhu, A., Shen, J., & Lin, S. (2004). Various approaches to modify biomaterial surfaces for improving hemocompatibility. *Advances in Colloid and Interface Science*, 110(1-2), 5-17.
- [8] Goddard, J. M., & Hotchkiss, J. H. (2007). Polymer surface modification for the attachment of bioactive compounds. *Progress in Polymer Science*, 32(7), 698-725.
- [9] Zanini, S., Riccardi, C., Grimoldi, E., Colombo, C., Villa, A. M., Natalello, A., ... & Doglia, S. M. (2010). Plasma-induced graft-polymerization of polyethylene glycol acrylate on polypropylene films: chemical characterization and evaluation of the protein adsorption. *Journal of Colloid and Interface Science*, 341(1), 53-58.
- [10] Kyomoto, M., Moro, T., Takatori, Y., Kawaguchi, H., Nakamura, K., & Ishihara, K. (2010). Self-initiated surface grafting with poly (2-methacryloyloxyethyl phosphorylcholine) on poly (ether-ether-ketone). *Biomaterials*, 31(6), 1017-1024.
- [11] Zhang, C., Qu, G., Sun, Y., Wu, X., Yao, Z., Guo, Q., ... & Zhou, H. (2008). Pharmacokinetics, biodistribution, efficacy and safety of N-octyl-O-sulfate chitosan micelles loaded with paclitaxel. *Biomaterials*, 29(9), 1233-1241.
- [12] Zhang, C., Qu, G., Sun, Y., Yang, T., Yao, Z., Shen, W., ... & Ping, Q. (2008). Biological evaluation of N-octyl-O-sulfate chitosan as a new nano-carrier of

intravenous drugs. *European Journal of Pharmaceutical sciences*, 33(4-5), 415-423.

- [13] Huang, X. J., Guduru, D., Xu, Z. K., Vienken, J., & Groth, T. (2011). Blood compatibility and permeability of heparin-modified polysulfone as potential membrane for simultaneous hemodialysis and LDL removal. *Macromolecular Bioscience*, 11(1), 131-140.
- [14] Sask, K. N., McClung, W. G., Berry, L. R., Chan, A. K., & Brash, J. L. (2011). Immobilization of an antithrombin–heparin complex on gold: Anticoagulant properties and platelet interactions. *Acta Biomaterialia*, 7(5), 2029-2034.
- [15] Yang, J., Cai, J., Wu, K., Li, D., Hu, Y., Li, G., & Du, Y. (2012). Preparation, characterization and anticoagulant activity in vitro of heparin-like 6-carboxylchitin derivative. *International Journal of Biological Macromolecules*, 50(4), 1158-1164.
- [16] Duraiswamy, N., Choksi, T. D., Pinchuk, L., & Schoepfoerster, R. T. (2009). A Phospholipid-modified Polystyrene—Polyisobutylene—Polystyrene (SIBS) Triblock Polymer for Enhanced Hemocompatibility and Potential Use in Artificial Heart Valves. *Journal of Biomaterials Applications*, 23(4), 367-379.
- [17] Seo, J. H., Matsuno, R., Konno, T., Takai, M., & Ishihara, K. (2008). Surface tethering of phosphorylcholine groups onto poly (dimethylsiloxane) through swelling–deswelling methods with phospholipids moiety containing ABA-type block copolymers. *Biomaterials*, 29(10), 1367-1376.

- [18] Xu, F., Nacker, J. C., Crone, W. C., & Masters, K. S. (2008). The haemocompatibility of polyurethane–hyaluronic acid copolymers. *Biomaterials*, 29(2), 150-160.
- [19] Williams, D. F. (2008). On the mechanisms of biocompatibility. *Biomaterials*, 29(20), 2941-2953.
- [20] Mao, C., Qiu, Y., Sang, H., Mei, H., Zhu, A., Shen, J., & Lin, S. (2004). Various approaches to modify biomaterial surfaces for improving hemocompatibility. *Advances in Colloid and Interface Science*, 110(1-2), 5-17.
- [21] Chen, H., Yuan, L., Song, W., Wu, Z., & Li, D. (2008). Biocompatible polymer materials: role of protein–surface interactions. *Progress in Polymer Science*, 33(11), 1059-1087.
- [22] Ratner, B. D., & Bryant, S. J. (2004). Biomaterials: where we have been and where we are going. *Annu. Rev. Biomed. Eng.*, 6, 41-75.
- [23] Anderson, J. M. (2001). Biological responses to materials. *Annual Review of Materials Research*, 31(1), 81-110.
- [24] Sivaraman, B., & Latour, R. A. (2010). The relationship between platelet adhesion on surfaces and the structure versus the amount of adsorbed fibrinogen. *Biomaterials*, 31(5), 832-839.

- [25] Deng, Z. J., Liang, M., Monteiro, M., Toth, I., & Minchin, R. F. (2011). Nanoparticle-induced unfolding of fibrinogen promotes Mac-1 receptor activation and inflammation. *Nature Nanotechnology*, 6(1), 39.
- [26] Agyare, E. K., Curran, G. L., Ramakrishnan, M., Caroline, C. Y., Poduslo, J. F., & Kandimalla, K. K. (2008). Development of a smart nano-vehicle to target cerebrovascular amyloid deposits and brain parenchymal plaques observed in Alzheimer's disease and cerebral amyloid angiopathy. *Pharmaceutical Research*, 25(11), 2674-2684.
- [27] Zhou, H. Y., Zhang, Y. P., Zhang, W. F., & Chen, X. G. (2011). Biocompatibility and characteristics of injectable chitosan-based thermosensitive hydrogel for drug delivery. *Carbohydrate Polymers*, 83(4), 1643-1651.
- [28] Langer, R., & Tirrell, D. A. (2004). Designing materials for biology and medicine. *Nature*, 428(6982), 487.
- [29] Abbasi, F., & Mirzadeh, H. A. M. I. D. (2004). Adhesion between modified and unmodified poly (dimethylsiloxane) layers for a biomedical application. *International Journal of Adhesion and Adhesives*, 24(3), 247-257.
- [30] Wnek, G. E., & Bowlin, G. L. (Eds.). (2008). *Encyclopedia of Biomaterials and Biomedical Engineering*. CRC Press.

- [31] Richey, T., Iwata, H., Oowaki, H., Uchida, E., Matsuda, S., & Ikada, Y. (2000). Surface modification of polyethylene balloon catheters for local drug delivery. *Biomaterials*, 21(10), 1057-1065.
- [32] Alferiev, I. S., Connolly, J. M., Stachelek, S. J., Ottey, A., Rauova, L., & Levy, R. J. (2006). Surface heparinization of polyurethane via bromoalkylation of hard segment nitrogens. *Biomacromolecules*, 7(1), 317-322.
- [33] Kingshott, P., Wei, J., Bagge-Ravn, D., Gadegaard, N., & Gram, L. (2003). Covalent attachment of poly (ethylene glycol) to surfaces, critical for reducing bacterial adhesion. *Langmuir*, 19(17), 6912-6921.
- [34] Hadjichristidis, N., Pitsikalis, M., Iatrou, H., Driva, P., Chatzichristidi, M., Sakellariou, G., & Lohse, D. (2002). Graft copolymers. *Encyclopedia of Polymer Science and Technology*.
- [35] Elkholy, S. S., Khalil, K. D., & Elsabee, M. Z. (2006). Homogeneous and heterogeneous grafting of 4-vinylpyridine onto chitosan. *Journal of Applied Polymer Science*, 99(6), 3308-3317.
- [36] M. Ishihara, M. Fujita, S. Kishimoto, H. Hattori & Y. Kanatani, Chitosan-Based Systems for Biopharmaceuticals: Delivery, Targeting and Polymer Therapeutics, in: B. Sarmiento, D.J. Neves (Eds), Biological, chemical, and physical compatibility of chitosan and biopharmaceuticals, John Wiley & Sons, Chichester, 2012, pp. 93-106.

- [37] Dumitriu, S. (2001). Chitosan: Structure–Properties Relationship and Biomedical Applications Alain Domard and Monique Domard. In *Polymeric Biomaterials, Revised and Expanded* (pp. 201-226). CRC Press.
- [38] M. Weber, H. Steinle, S. Golombek, L. Hann, C. Schlensak, H. P. Wendel, M. Avci-Adal, Blood-Contacting Biomaterials: In Vitro Evaluation of the Hemocompatibility, *Frontiers in Bioengineering and Biotechnology*, 6 (2018) 99. <https://doi.org/10.3389/fbioe.2018.00099>
- [39] Z. Hu, D.Y. Zhang, S.T. Lu, P.W. Li, S.D. Li, Chitosan-Based Composite Materials for Prospective Hemostatic Applications, *Marine Drugs*. 16. 8 (2018) 273. <https://doi.org/10.3390/md16080273>
- [40] Balan, V., & Verestiuc, L. (2014). Strategies to improve chitosan hemocompatibility: A review. *European Polymer Journal*, 53, 171-188. <https://doi.org/10.1016/j.eurpolymj.2014.01.033>
- [41] W.G. Malette, H.J. Quigley, R.D. Gaines, N.D. Johnson, W.G. Rainer, Chitosan: a new hemostatic, *The Annals of Thoracic Surgery*. 36 (1986), 55–58. [https://doi.org/10.1016/S0003-4975\(10\)60649-2](https://doi.org/10.1016/S0003-4975(10)60649-2)
- [42] P.R. Klokkevold, D.S. Lew, D.G. Ellis, C.N. Bertolami, Effects of chitosan on lingual hemostasis in rabbits, *Journal of Oral and Maxillofacial Surgery*. 49.8 (1991) 858–863. [https://doi.org/10.1016/0278-2391\(91\)90017-G](https://doi.org/10.1016/0278-2391(91)90017-G)

- [43] T.C. Chou, E. Fu, C.J. Wu, J.H. Yeh, Chitosan enhances platelet adhesion and aggregation, *Biochemical and Biophysical Research Communications*. 302 (2003) 480-483. [https://doi.org/10.1016/S0006-291X\(03\)00173-6](https://doi.org/10.1016/S0006-291X(03)00173-6)
- [44] V. Balan, I.A. Petrache, M.I. Popa, M. Butnaru, E. Barbu, J. Tsibouklis, L. Verestiuc, Biotinylated chitosan-based SPIONs with potential in blood contacting applications, *Journal of Nanoparticle Research*. 14 (2014) 730–43. <https://doi.org/10.1007/s11051-012-0730-y>
- [45] W. Y. Xiong, Y. Yi, H. Z. Liu, H. Wang, J. H. Liu, G. Q. Ying, Selective carboxypropionylation of chitosan: synthesis, characterization, blood compatibility, and degradation, *Carbohydrate Research*. 346 (2011) 1217–1223. <https://doi.org/10.1016/j.carres.2011.03.037>
- [46] S. Meng, Z. Liu, W. Zhong, Q. Wang, Q. Du, Phosphorylcholine modified chitosan: appetent and safe material for cells, *Carbohydrate Polymers*, 70 (2007), 82–88. <https://doi.org/10.1016/j.carbpol.2007.03.006>
- [47] Z. Yalinca, Y. Yilmaz, B. Taneri, F. Bullici, S. Tuzmen, Blood contact properties of ascorbyl chitosan, *Journal of Biomaterials Science, Polymer Edition*. 24 (2017) 1969-1987. <https://doi.org/10.1080/09205063.2013.816929>
- [48] Bader, H. J., & Birkholz, E. (1997). Teaching chitin chemistry. *Chitin handbook*. RAA Muzzarelli and MG Peter (Eds.). *European Chitin Society. Atec. Grottammare. Italy*, 507-519.


- [49] Bhatia, S. C., & Ravi, N. (2000). A magnetic study of an Fe⁻ chitosan complex and its relevance to other biomolecules. *Biomacromolecules*, 1(3), 413-417.
- [50] Guibal, E., Milot, C., Roussy, J., Bader, H. J., & Birkholz, E. (1997). Chitin Handbook. *European Chemical Society*, 423.
- [51] Weltrowski, M., Martel, B., & Morcellet, M. (1996). Chitosan N-benzyl sulfonate derivatives as sorbents for removal of metal ions in an acidic medium. *Journal of Applied Polymer Science*, 59(4), 647-654.
- [52] Burke, A., Yilmaz, E., Hasirici, N. (2000). Evaluation of chitosan as a potential medical iron (III) ion adsorbent. *Turkish Journal of Medical Sciences*, 30(4), 341-348.
- [53] Dalsin, J. L., & Messersmith, P. B. (2005). Bioinspired antifouling polymers. *Materials Today*, 8(9), 38-46.
- [54] Zhao, C., & Zheng, J. (2011). Synthesis and characterization of poly (N-hydroxyethylacrylamide) for long-term antifouling ability. *Biomacromolecules*, 12(11), 4071-4079.
- [55] Zhao, C., Li, X., Li, L., Cheng, G., Gong, X., & Zheng, J. (2013). Dual functionality of antimicrobial and antifouling of poly (N-hydroxyethylacrylamide)/salicylate hydrogels. *Langmuir*, 29(5), 1517-1524.

- [56] Rodriguez-Emmenegger, C., Houska, M., Alles, A. B., & Brynda, E. (2012).
Surfaces resistant to fouling from biological fluids: towards bioactive surfaces
for real applications. *Macromolecular Bioscience*, 12(10), 1413-1422.

APPENDIX

Appendix A: Ethical Consent





EK: 542-207


YAKIN DOĞU ÜNİVERSİTESİ
BİLİMSEL ARAŞTIRMALAR DEĞERLENDİRME ETİK KURULU

ARAŞTIRMA PROJESİ DEĞERLENDİRME RAPORU

Toplantı Tarihi : 17.08.2017
Toplantı No : 2017/49
Proje No : 438

Yakın Doğu Üniversitesi Mühendislik Fakültesi öğretim üyelerinden Doç. Dr. Terin Adalı'nın sorumlu araştırmacısı olduğu, YDU/2017/49-438 proje numaralı ve "Kitosan/Poli (N-Hidroksietil Akrilamid) Hidrojellerin Kan Uyumluluğunun Araştırılması" başlıklı proje önerisi kurulumuzca değerlendirilmiş olup, etik olarak uygun bulunmuştur.

1. Prof. Dr. Rüştü Onur	(BAŞKAN) 
2. Prof. Dr. Nerin Bahçeciler Önder	(ÜYE) KATILMIYADI
3. Prof. Dr. Tamer Yılmaz	(ÜYE) KATILMIYADI
4. Prof. Dr. Şahan Saygı	(ÜYE) KATILMIYADI
5. Prof. Dr. Şanda Çalı	(ÜYE) KATILMIYADI
6. Prof. Dr. Nedim Çakır	(ÜYE) KATILMIYADI
7. Prof. Dr. Kaan Erler	(ÜYE) 
8. Doç. Dr. Ümran Dal Yılmaz	(ÜYE) KATILMIYADI
9. Doç. Dr. Eyüp Yayı	(ÜYE) 
10. Doç. Dr. Nilüfer Galip Çelik	(ÜYE) 
11. Yrd. Doç. Dr. Emil Mammadov	(ÜYE) 